

# Four-point correlators of BPS operators in $\mathcal{N} = 4$ SYM at order $g^4$

G.Arutyunov<sup>(a)</sup>, S. Penati<sup>(b)</sup>, A. Santambrogio<sup>(c)</sup>, E. Sokatchev<sup>(d)</sup>

<sup>(a)</sup> *Max-Planck-Institut für Gravitationsphysik, Albert-Einstein-Institut,  
Am Mühlenberg 1, D-14476 Golm, Germany*

<sup>(b)</sup> *Dipartimento di Fisica, Università degli studi di Milano-Bicocca and INFN, Sezione di Milano,  
piazza della Scienza 3, I-20126 Milano, Italy*

<sup>(c)</sup> *Dipartimento di Fisica, Università degli studi di Milano and INFN, Sezione di Milano, via  
Celoria 16, I-20133 Milano, Italy*

<sup>(d)</sup> *Laboratoire d'Annecy-le-Vieux de Physique Théorique<sup>1</sup> LAPTH, B.P. 110, F-74941  
Annecy-le-Vieux, France*

## ABSTRACT

We study the large  $N$  degeneracy in the structure of the four-point amplitudes of  $\frac{1}{2}$ -BPS operators of arbitrary weight  $k$  in perturbative  $\mathcal{N} = 4$  SYM theory. At one loop (order  $g^2$ ) this degeneracy manifests itself in a smaller number of independent conformal invariant functions describing the amplitude, compared to AdS<sub>5</sub> supergravity results. To study this phenomenon at the two-loop level (order  $g^4$ ) we consider a particular  $\mathcal{N} = 2$  hypermultiplet projection of the general  $\mathcal{N} = 4$  amplitude. Using the formalism of  $\mathcal{N} = 2$  harmonic superspace we then explicitly compute this four-point correlator at two loops and identify the corresponding conformal invariant functions.

In the cases of  $\frac{1}{2}$ -BPS operators of weight  $k = 3$  and  $k = 4$  the one-loop large  $N$  degeneracy is lifted by the two-loop corrections. However, for weight  $k > 4$  the degeneracy is still there at the two-loop level. This behavior suggests that for a given weight  $k$  the degeneracy will be removed if perturbative corrections of sufficiently high order are taken into account. These results are in accord with the AdS/CFT duality conjecture.

PACS: 03.70.+k, 11.15.-q, 11.10.-z, 11.30.Pb, 11.30.Rd

Keywords: AdS/CFT, SYM theory, Anomalous dimensions, Superspace.

---

<sup>1</sup>UMR 5108 associée à l'Université de Savoie

# 1 Introduction

In recent years the supersymmetric quantum conformal field theories in dimensions higher than two have undergone a renaissance due to the discovery of the AdS/CFT correspondence [1]. In the first place this concerns  $\mathcal{N} = 4$  super Yang-Mills (SYM) theory in four dimensions whose conjectured dual is type IIB (superstring) supergravity on an anti-de Sitter background.

On the string theory side the present investigations are focused either on low-energy supergravity or on semiclassical string solutions carrying non-vanishing global charges of the superconformal group. In the latter case a direct comparison of the corresponding string energies to the spectrum of scaling dimensions of certain composite operators in  $\mathcal{N} = 4$  SYM is possible [2, 3, 4].

According to the duality conjecture, AdS supergravity is dual to the gauge theory taken at an infinite value of the 't Hooft coupling  $\lambda$  and in the large  $N$  limit, where  $N$  is the rank of the gauge group (S)U( $N$ ). In this limit the gauge theory reveals the following peculiar behavior:

- the sector of protected operators is enlarged;
- the spectrum of anomalous dimensions degenerates;
- the symmetry is enhanced.

The first property is a simple consequence of the rather general fact that in the large  $N$  limit the anomalous dimension of a multi-trace operator made of single-trace constituents is equal to the sum of their individual anomalous dimensions. In this sense, in the large  $N$  limit the protected operators form a ring<sup>1</sup>.

The second property is more subtle and it is reminiscent of the free theory pattern, where usually several operators with the same canonical dimension coexist. It is well known that protected (for instance,  $\frac{1}{2}$ -BPS) operators with the same quantum numbers can be realized in the gauge theory both as single- and multi-trace operators. Thus, multiplying protected operators with the same quantum numbers by an unprotected operator, we obtain different operators with the same dimension in the planar limit, hence the degenerate spectrum. Such a mechanism is essentially due to the conformal supersymmetry responsible for the protection and, again, due to the large  $N$  factorization property of the Feynman graphs. However, this is not the whole story. As was recently shown in Ref. [5], there exist, for instance, single-trace operators (which cannot be obtained as the product of a protected and an unprotected operators) whose anomalous dimensions coincide up to two loops. This is evidence for an extra symmetry in the planar limit which is responsible for this degeneracy of the perturbative spectrum. The symmetry enhancement [5] is an interesting property of the gauge theory related, for instance, to the integrability of the spin chain Hamiltonian [6]. The latter can be identified with the one-loop dilatation operator in  $\mathcal{N} = 4$  SYM.

Recently, another interesting peculiarity of the large  $N$  limit of  $\mathcal{N} = 4$  SYM was found [7]. We recall that in regard to the supergravity approximation of the gauge theory, the

---

<sup>1</sup>When computing the two-point function of a multi-trace operator, one can readily see that the leading  $1/N$  contribution is due to the Feynman graphs which contribute separately to the two-point functions of the individual single-trace constituents.

most interesting object to study are the four-point correlation functions of  $\frac{1}{2}$ -BPS operators (for reviews see, e.g. [8, 9]). These operators are dual to the Kaluza-Klein states of the compactified type IIB supergravity. They form isolated series of superconformal representations and their scaling dimension as well as their two- and three-point correlation functions are protected from receiving quantum corrections. In contrast, their four-point correlators undergo perturbative renormalization.

The four-point amplitude of  $\frac{1}{2}$ -BPS operators with arbitrary weights (dimensions)  $k_p$ ,  $p = 1, 2, 3, 4$  is specified by a number of conformal invariant functions depending on the two conformal cross-ratios. There is a general procedure based on the field-theoretic insertion formula which allows one to determine the maximal number of *a priori* independent such functions appearing in the quantum part of the amplitude [10, 11].

The explicit amplitudes corresponding to the cases where all  $k_p \equiv k$  are equal to 2, 3 or 4 have been computed in the supergravity approximation by using the effective five-dimensional description of type IIB, and also in perturbation theory at one loop (order  $g^2$ ) and in the planar limit. It was then observed in Ref. [7] that the perturbative amplitudes exhibit a certain degeneracy in comparison to their supergravity counterparts. Starting from  $k = 4$ , the number of conformal invariant functions describing the amplitude at one loop is smaller than in the supergravity regime. We can formulate this fact as another interesting property of the large  $N$  limit:

- the perturbative four-point amplitudes of  $\frac{1}{2}$ -BPS operators degenerate.

Thus, not only the two-point functions (the spectrum) but also the higher-point perturbative amplitudes exhibit simplified features in the large  $N$  limit.

The aim of the present paper is to study this degeneracy in more detail. Recall that for the first time the degenerate situation occurs for  $k = 4$ . In the supergravity regime one finds two different conformal invariant functions, precisely the number predicted on general grounds. However, at one loop the two functions describing the large  $N$  amplitude coincide. It should be noted that the perturbative computation has been performed for  $\frac{1}{2}$ -BPS operators realized as *single-trace* operators. Generically, the  $\frac{1}{2}$ -BPS operators can be realized as mixtures of single- and multi-trace operators with arbitrary mixing coefficients. Therefore, two natural questions can be asked about this large  $N$  degeneracy:

1. *Does the operator mixing influence the degeneracy?*
2. *Is the degeneracy lifted when the higher-loop corrections are taken into account?*

We study the first question by using the  $k = 4$  amplitude as the simplest example. The  $\frac{1}{2}$ -BPS operator of dimension 4 is a mixture of one single- and one double-trace operator, the latter is made of two single-trace constituents of dimension 2. Firstly, we show that the free amplitude involving mixed operators coincides with that for single traces in the large  $N$  limit, provided that the mixing parameter scales faster than  $1/\sqrt{N}$ . As discussed in Ref. [7], the supergravity-induced amplitude admits a *unique splitting* into a “constant” and an “interacting” parts. The former precisely matches the free amplitude computed for single-trace operators. In the AdS/CFT language the interacting part must comprise all loop corrections to the free amplitude. Clearly, in order not to affect this agreement with the constant part of the supergravity amplitude, in field theory we should allow only mixing which is more heavily suppressed than  $1/\sqrt{N}$ . Secondly, we argue that with such a mixing

the contribution of the double-trace operators at one loop is suppressed in the large  $N$  limit as well, so the degeneracy is not affected by the operator mixing.

We then investigate the issue of the higher-loop corrections by extending the perturbative treatment to two loops (order  $g^4$ ). To illustrate the more general picture, we consider the amplitude involving  $\frac{1}{2}$ -BPS operators of equal but arbitrary weight  $k$ . By performing an explicit diagrammatic computation we find that at two loops the degeneracy occurring in the case  $k = 4$  is lifted: Two different conformal invariant functions emerge. However, for amplitudes involving operators of weight  $k > 4$  the degeneracy persists even at the two-loop level. These observations indicate that for a fixed weight  $k$  the degeneracy is removed when loop corrections of sufficiently high order (depending on  $k$ ) are taken into account. Since the supergravity-induced amplitudes comprise all perturbative corrections, it is natural to expect them to realize the maximal possible number of different conformal invariants.

In fact, the perturbative degeneracy phenomenon has a rather simple origin. At a given order of perturbation theory we have only a finite number of topologically different planar interacting graphs. Whether all of them are indeed present depends on the weight  $k$  of the four composite operators for which the amplitude is computed. It is clear that increasing  $k$  makes all possible interacting topologies appear. Eventually, we reach the point of saturation beyond which increasing the weight amounts to decorating the interacting graphs with free propagators. In the large  $N$  limit this does not generate new conformal invariants. On the contrary, fixing  $k$  and increasing the order of perturbation theory “awakes” new interacting topologies and hence generates new conformal invariants, thus lifting the degeneracy.

One could also ask if there is any relationship between the degeneracy of the four-point amplitudes and that of the spectrum observed in Ref. [5]. Any conformal invariant function can be expanded over an infinite basis of conformal partial wave amplitudes, each of which represents the contributions of an individual primary operator. The degeneracy of the four-point functions is therefore related to some kind of degeneracy of the spectrum and of the OPE coefficients. It would be interesting to find out if the degeneracy of the spectrum is also removed when higher loop corrections are taken into account. Indeed, in the lattice picture [6] the  $L$ -loop dilatation matrix induces the mixing of the  $L+1$  neighboring elementary fields constituting a composite operator, i.e. with  $L$  growing the effective interaction is spreading over the lattice and can subsequently increase its size which is equal to the dimension of the operator. When this happens, the degeneracy might be lifted in a way similar to that for the four-point amplitudes.

The organization of the paper is as follows. In Section 2 we describe the structure of the  $\mathcal{N} = 4$  four-point amplitude of  $\frac{1}{2}$ -BPS operators determined by the field-theoretic insertion procedure and discuss its “pure”  $\mathcal{N} = 2$  hypermultiplet projection. It involves a subset of  $k - 2$  conformal invariant functions (or one such function for  $k = 2$ ) from the original  $\mathcal{N} = 4$  amplitude. For  $k > 4$  this subset is not complete but it is sufficiently large to illustrate the degeneracy problem. The advantage of the hypermultiplet projection is that we can use the quantum formalism of  $\mathcal{N} = 2$  off-shell harmonic superspace [12] which is particularly efficient at two loops<sup>2</sup>. For the sake of clarity, at the end of Section 2 we present and discuss our main results, whose derivation is explained in detail in Sections 4 and 5. In Section 3 we discuss the influence of operator mixing on the degeneracy problem. In Section 4 we summarize the  $\mathcal{N} = 2$  insertion procedure and the Feynman diagram tools necessary to perform the two-

---

<sup>2</sup>Correlation functions of  $\frac{1}{2}$ -BPS operators at order  $g^4$  have also been computed in the  $\mathcal{N} = 1$  superspace formalism [13, 14].

loop computation of the hypermultiplet projection. In Section 5 a diagrammatic calculation is presented and the corresponding conformal invariants are identified. Finally, in Section 6 we use the operator product expansion and the knowledge of the one-loop anomalous dimensions of certain operators to get an insights into the structure of the  $k = 3$  and  $k = 4$  amplitudes, independently of the diagrammatics. In particular, for  $k = 3$  we are able to completely reconstruct the two-loop amplitude from these OPE considerations. Appendix A clarifies the technical tool of harmonic analyticity which we systematically use in order to drastically reduce the number of relevant Feynman graphs. Appendix B contains the details of the graph calculation for  $k = 3$  and 4 whose generalization for arbitrary  $k$  is given in Section 5.

## 2 Generalities and main result

The lowest component of a  $\frac{1}{2}$ -BPS multiplet in  $\mathcal{N} = 4$  SYM is a real scalar field of dimension  $k$  transforming in the irrep  $[0, k, 0]$  of the R symmetry group  $SO(6) \sim SU(4)$ . In terms of the elementary fields it can be realized, e.g., as a single-trace operator

$$\text{Tr}(\phi^{\{a_1} \dots \phi^{a_n\}}). \quad (2.1)$$

Here  $\phi^a$ ,  $a = 1, \dots, 6$  are the  $\mathcal{N} = 4$  SYM scalars and  $\{, \}$  denotes traceless symmetrization. A convenient way to handle the  $SO(6)$  indices is to project the operator (2.1) onto the highest weight state of the irrep  $[0, k, 0]$ . This can be done with the help of a complex null vector  $u^a$  ( $u^a u^a = 0$ ) carrying  $U(1)$  charge, which can be viewed as a harmonic variable parametrizing the coset space  $SO(6)/SO(2) \times SO(4)$  (see, e.g., Ref. [10] for details):

$$\mathcal{O}^{(k)} = u^{a_1} \dots u^{a_k} \text{Tr}(\phi^{a_1} \dots \phi^{a_k}). \quad (2.2)$$

We start by summarizing the general properties of the four-point amplitude of  $\frac{1}{2}$ -BPS operators in the  $\mathcal{N} = 4$  SYM theory. It is sufficient to restrict our discussion to the case where all the operators involved have equal weights  $k$ . On the basis of conformal and R symmetry alone the general form of the four-point amplitude can be parametrized as follows:

$$\langle k|k|k|k \rangle = \sum_{m+n+l=k} a_{mnl}^{(k)}(s, t) \mathcal{X}^m \mathcal{Y}^n \mathcal{Z}^l, \quad (2.3)$$

where  $m, n, l$  are non-negative integers. This expression is a polynomial in the three elementary propagator (Wick) contractions of the four points

$$\mathcal{X} = \frac{(12)(34)}{x_{12}^2 x_{34}^2}, \quad \mathcal{Y} = \frac{(13)(24)}{x_{13}^2 x_{24}^2}, \quad \mathcal{Z} = \frac{(14)(23)}{x_{14}^2 x_{23}^2}. \quad (2.4)$$

Here  $(12) = (21) \equiv u_1^a u_2^a$ , etc. denote the  $SO(6)$  invariant contractions of the harmonic variables at two different points. Every monomial in eq. (2.3) corresponds to a certain propagator structure built out of the propagators of the elementary fields (see Fig. 1). We refer to eq. (2.3) as to the representation of the amplitude in the propagator basis. The coefficients  $a_{mnl}^{(k)}(s, t)$  are arbitrary functions of the two independent conformal invariant cross-ratios

$$s = \frac{x_{12}^2 x_{34}^2}{x_{13}^2 x_{24}^2}, \quad t = \frac{x_{14}^2 x_{23}^2}{x_{13}^2 x_{24}^2}.$$

Superconformal symmetry puts additional kinematical restrictions on the coefficient functions in (2.3) which take the form of differential equations (superconformal Ward identities) [15, 16]. Further, dynamical constraints on the amplitude are obtained through the procedure of inserting the  $\mathcal{N} = 2$  SYM action. According to the “partial non-renormalization theorem” of Ref. [17], the quantum  $\mathcal{N} = 2$  amplitude takes a *factorized form* (see Section 4 for details). Recently this insertion procedure has been generalized to the  $\mathcal{N} = 4$  case [10, 7]. The factorized form of the quantum corrections to the  $\mathcal{N} = 4$  amplitude is

$$\langle k|k|k|k \rangle^{\text{quant.}} = R_{\mathcal{N}=4} \sum_{m+n+l=k-2} \mathcal{F}_{mnl}^{(k)}(s, t) \mathcal{X}^m \mathcal{Y}^n \mathcal{Z}^l, \quad (2.5)$$

where  $R_{\mathcal{N}=4}$  is a *universal polynomial prefactor* carrying weight 2 at each point. Explicitly,

$$\begin{aligned} R_{\mathcal{N}=4} = & s \mathcal{X}^2 + \mathcal{Y}^2 + t \mathcal{Z}^2 + (s - t - 1) \mathcal{Y}\mathcal{Z} \\ & + (1 - s - t) \mathcal{X}\mathcal{Z} + (t - s - 1) \mathcal{X}\mathcal{Y}. \end{aligned} \quad (2.6)$$

All the dynamical information is thus encoded in the conformally invariant coefficient functions  $\mathcal{F}_{mnl}^{(k)}(s, t)$  which are the subject of our subsequent investigation.<sup>3</sup> Substituting the universal prefactor into eq. (2.5) and comparing it with eq. (2.3), we read off the following expression for the *quantum corrections* to the coefficients  $a_{mnl}^{(k)}$ :

$$\begin{aligned} a_{mnl}^{(k)}(s, t) = & s \mathcal{F}_{m-2, n, l}^{(k)} + \mathcal{F}_{m, n-2, l}^{(k)} + t \mathcal{F}_{m, n, l-2}^{(k)} \\ & + (s - t - 1) \mathcal{F}_{m, n-1, l-1}^{(k)} + (1 - s - t) \mathcal{F}_{m-1, n, l-1}^{(k)} + (t - s - 1) \mathcal{F}_{m-1, n-1, l}^{(k)}. \end{aligned} \quad (2.7)$$

If any of the indices of  $\mathcal{F}_{mnl}^{(k)}$  in this equation becomes negative, then the corresponding term is absent.

Since all the operators involved are identical, the four-point amplitude is invariant under the symmetric group  $S_4$  which permutes the points  $1, \dots, 4$ . Only the subgroup  $S_3$  acts non-trivially on the cross-ratios  $s$  and  $t$  and, as a result, on the coefficient functions  $\mathcal{F}_{mnl}^{(k)}$ . It is generated by the two independent crossing transformations, e.g.,  $1 \leftrightarrow 2$  and  $1 \leftrightarrow 3$ . If all the indices  $m, n, l$  of  $\mathcal{F}_{mnl}^{(k)}$  are different, one can use the action of  $S_3$  to order them, e.g.,  $m > n > l$ . The function  $\mathcal{F}_{mnl}^{(k)}$  with  $m > n > l$  does not satisfy any crossing symmetry relation. It can be taken as a representative of the corresponding crossing equivalence class consisting of six elements. If any two indices of  $\mathcal{F}_{mnl}^{(k)}$  coincide, then the function satisfies an additional crossing symmetry relation (and the corresponding crossing equivalence class consists of three elements). Finally, in the case where all three indices coincide, the function transforms into itself under the whole group  $S_3$  (and the corresponding crossing equivalence class consists of a single element).

---

<sup>3</sup>To make the reader familiar with the notation we stress that the upper index in  $\mathcal{F}_{mnl}^{(k)}(s, t)$  denotes the weight of the  $\frac{1}{2}$ -BPS operators. For the sake of clarity we sometimes separate the lower indices by commas.

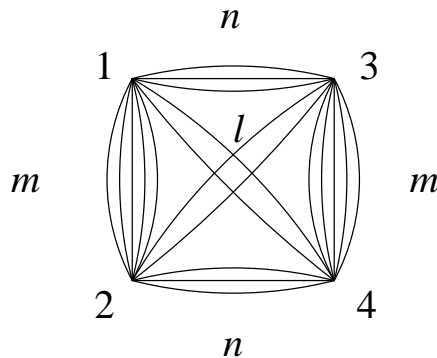


Figure 1. The propagator structure corresponding to the monomial  $\mathcal{X}^m \mathcal{Y}^n \mathcal{Z}^l$ .

For sufficiently small values of  $k$  the number of conformal invariants  $\mathcal{F}$  representing the independent crossing equivalence classes is easy to work out (the general formula is given in Ref. [11]). For instance, both for  $k = 2, 3$  the quantum part of the amplitude is given by a single function  $\mathcal{F}$ , while already for  $k = 4$  two functions are needed.

The functions  $\mathcal{F}$  can be explicitly computed both in perturbation theory and in the strong coupling regime by using the AdS/CFT duality. In Ref. [7] it was observed that in the large  $N$  limit the perturbative four-point amplitudes of the  $\frac{1}{2}$ -BPS operators exhibit a certain *degenerate behavior* in comparison to their supergravity partners: The number of independent conformal invariants describing the one-loop (order  $\lambda \sim g^2$ ) perturbative amplitude is smaller than that in the supergravity regime. In what follows we study this degeneracy phenomenon at the two-loop (order  $\lambda^2 \sim g^4$ ) level by explicitly working out the corresponding four-point amplitude.

Computing four-point correlation functions at two loops is of course much more involved than at one loop, due to the rapidly increasing number of Feynman graphs. A very efficient technique is provided by the  $\mathcal{N} = 2$  harmonic superspace formalism. This approach, combined with the  $\mathcal{N} = 2$  insertion procedure, allows us to drastically reduce the number of relevant graph topologies to be computed.

In order to apply the  $\mathcal{N} = 2$  harmonic superspace formalism we need to decompose the  $\frac{1}{2}$ -BPS operators into their  $\mathcal{N} = 2$  hypermultiplet (HM) and SYM constituents. This is done by first decomposing the  $\mathcal{N} = 4$  field-strength superfield  $\mathcal{W} = u^a \phi^a(x) + \dots$  into the Grassmann analytic HM superfield  $q^+ = u_i^+ \phi^i(x) + \dots$  (and its harmonic conjugate<sup>4</sup>  $\tilde{q}^+ = u_i^+ \bar{\phi}^i(x) + \dots$ ) and the chiral field strength  $W = w(x) + \dots$  (and its antichiral conjugate  $\bar{W} = \bar{w}(x) + \dots$ ). Here the six real scalars  $\phi^a(x)$  forming an  $\text{SO}(6)$  vector have been split into an  $\text{SU}(2)$  doublet  $\phi^i(x)$ ,  $i = 1, 2$  and a complex singlet  $w(x)$ . The  $\text{SO}(6)$  vector harmonics  $u^a$  have been replaced by  $\text{SU}(2)$  fundamental harmonics  $u_i^\pm$  ( $u^- = (u^+)^*$ ,  $u_i^+ \epsilon^{ij} u_j^- = 1$ ), parametrizing the sphere  $S^2 \sim \text{SU}(2)/\text{U}(1)$ .

In the sequel we will be interested in the “pure” HM projection in which we put only  $\tilde{q}$ ’s at points 1 and 4 and only  $q$ ’s at points 2 and 3. As explained in Ref. [7], taking this projection means considering only the terms with  $l = 0$  in eq. (2.3) (in Fig. 1 they correspond to the graphs without diagonals). Further, the propagator structures (2.4) are

<sup>4</sup>Here  $\tilde{q}$  means the usual complex conjugation for the field together with an antipodal reflection on the sphere  $S^2 \sim \text{SU}(2)/\text{U}(1)$  for the harmonic variable.

replaced by

$$\mathcal{X} \rightarrow X = \frac{[12][43]}{x_{12}^2 x_{34}^2}, \quad \mathcal{Y} \rightarrow Y = \frac{[13][42]}{x_{13}^2 x_{24}^2}, \quad (2.8)$$

where, e.g.,

$$[12] = -[21] \equiv (u_1)_i^+ \epsilon^{ij} (u_2)_j^+ \quad (2.9)$$

is the SU(2) invariant contraction of the two sets of harmonic variables at points 1 and 2. Under this projection eq. (2.5) reduces to

$$\langle Q^{(k)} \rangle \equiv \langle \tilde{q}^k | q^k | q^k | \tilde{q}^k \rangle = R_{\mathcal{N}=2} \sum_{m=0}^{k-2} \mathcal{F}_{m,k-m-2,0}^{(k)}(s,t) X^m Y^{k-m-2}, \quad (2.10)$$

where

$$R_{\mathcal{N}=2} = sX^2 + (t-s-1)XY + Y^2. \quad (2.11)$$

The factorized expression (2.10) with the universal prefactor (2.11) is precisely what one finds by the direct application of the field-theoretic insertion procedure to the four-point amplitude in the  $\mathcal{N} = 2$  theory (see Section 4).

According to the previous discussion of the crossing symmetry, we can take  $\mathcal{F}_{m,k-m-2,0}^{(k)}$  with

$$m_- \equiv 1/2(k-2) \leq m \leq k-2 \equiv m_+ \quad \text{for } k \text{ even} \quad (2.12)$$

and

$$1/2(k-1) \leq m \leq k-2 \equiv m_+ \quad \text{for } k \text{ odd} \quad (2.13)$$

as representatives of the different crossing equivalence classes of the coefficient functions of the four-point amplitude.

It should be pointed out that for  $k > 4$  the whole  $\mathcal{N} = 4$  amplitude cannot be restored from its pure  $\mathcal{N} = 2$  projection<sup>5</sup> and consequently, the functions  $\mathcal{F}_{m,k-m-2,0}^{(k)}$  above do not form a complete set of *a priori* independent conformal invariants needed to parametrize the amplitude. However, the subset of conformal invariants emerging in the pure HM projection is sufficiently large to illustrate the large  $N$  degeneracy problem at the two-loop level.

Among the chosen set of independent coefficient functions only one (for  $k$  odd) or two (for  $k$  even) admit a pair of coincident indices. The first such function  $\mathcal{F}_+^{(k)}(s,t) \equiv \mathcal{F}_{k-2,0,0}(s,t)$  is obtained by setting  $m = m_+$ , so it exists for any value of  $k$ .<sup>6</sup> It has the additional symmetry property

$$\mathcal{F}_+^{(k)}(s,t) = 1/t \mathcal{F}_+^{(k)}(s/t, 1/t). \quad (2.14)$$

<sup>5</sup>To this end we would also need some of the ‘‘mixed’’ projections of the type  $\tilde{q}^{k-p} q^p$ . Obtaining such projections involves some amount of linear algebra; in addition, the corresponding two-loop graphs are more complicated. Therefore here we prefer to restrict ourselves to the ‘‘pure’’ sector.

<sup>6</sup>One could instead take  $\mathcal{F}_{0,k-2,0}^{(k)}$  which obeys  $\mathcal{F}_{0,k-2,0}^{(k)}(s,t) = \mathcal{F}_{0,k-2,0}^{(k)}(t,s)$ . The relation between the two functions is  $\mathcal{F}_{k-2,0,0}^{(k)}(s,t) = 1/s \mathcal{F}_{0,k-2,0}^{(k)}(1/s, t/s)$ .

The second function  $\mathcal{F}_{m_-,m_-,0}^{(k)}$  is obtained by setting  $m = m_-$ , so it exists only for  $k$  even. In this case we have

$$\mathcal{F}_{m_-,m_-,0}^{(k)}(s,t) = 1/s \mathcal{F}_{m_-,m_-,0}^{(k)}(1/s, t/s). \quad (2.15)$$

It is more convenient to introduce the functions

$$\mathcal{F}_m^{(k)}(s,t) \equiv \mathcal{F}_{m,k-m-2,0}^{(k)}(t,s), \quad m \neq m_+ \quad (2.16)$$

since for  $m = m_-$  the function  $\mathcal{F}_-^{(k)}(s,t) \equiv \mathcal{F}_{m_-,m_-,0}^{(k)}(t,s)$  has the same crossing symmetry as  $\mathcal{F}_+^{(k)}$ :

$$\mathcal{F}_\pm^{(k)}(s,t) = 1/t \mathcal{F}_\pm^{(k)}(s/t, 1/t). \quad (2.17)$$

The functions  $\mathcal{F}_m^{(k)}$  with  $m_- < m < m_+$  do not a priori obey any crossing symmetry relations. Finally, we note that the case  $k = 2$  is exceptional as all the three indices of  $\mathcal{F}^{(2)}$  vanish. This function transforms covariantly under the whole group  $S_3$ .

In summary, the pure HM projection is parametrized by the chain of conformally invariant functions  $\mathcal{F}_m^{(k)}$  whose ‘‘boundaries’’  $\mathcal{F}_\pm^{(k)}$  are subject to the crossing symmetry relation (2.17). The function  $\mathcal{F}_-^{(k)}$  exists only for  $k$  even.

Concluding this section, we give the main result of our two-loop calculation, the details of which are presented in Sections 4 and 5. In the large  $N$  limit we find

$$\begin{aligned} \mathcal{F}_-^{(k)}(s,t) &= \frac{\lambda^2 k^2}{N^2} \frac{1}{4} \left\{ \frac{1}{4} s [\Phi^{(1)}(s,t)]^2 + \frac{1}{s} \Phi^{(2)}(t/s, 1/s) \right\} = \mathcal{F}_m^{(k)}(s,t), \\ \mathcal{F}_+^{(k)}(s,t) &= \frac{\lambda^2 k^2}{N^2} \frac{1}{4} \left\{ \frac{1}{4} (t+1) [\Phi^{(1)}(s,t)]^2 + \Phi^{(2)}(s,t) + \frac{1}{t} \Phi^{(2)}(s/t, 1/t) \right\}, \end{aligned} \quad (2.18)$$

where the range of  $m$  is given by Eqs. (2.12) and (2.13), in particular, for  $k$  odd the function  $\mathcal{F}_-^{(k)}$  is absent. In eqs. (2.18)  $\lambda = g^2 N / 4\pi^2$  is the 't Hooft coupling and the functions  $\Phi^{(1)}$  and  $\Phi^{(2)}$  are the so-called one- and two-loop scalar box conformal integrals

$$\int \frac{d^4 x_5}{x_{15}^2 x_{25}^2 x_{35}^2 x_{45}^2} \equiv -\frac{i\pi^2}{x_{13}^2 x_{24}^2} \Phi^{(1)}(s,t), \quad (2.19)$$

$$\int \frac{x_{13}^2 d^4 x_5 d^4 x_6}{x_{15}^2 x_{25}^2 x_{35}^2 x_{56}^2 x_{16}^2 x_{36}^2 x_{46}^2} \equiv \frac{(i\pi^2)^2}{x_{13}^2 x_{24}^2} \Phi^{(2)}(s,t). \quad (2.20)$$

We see that *in the large  $N$  limit all but one conformal invariants describing the pure HM projection are equal*. It is only the ‘‘boundary’’ function  $\mathcal{F}_+^{(k)}$  which is distinctly different from the others.

Having found the pure HM part of the four-point amplitude of the  $\frac{1}{2}$ -BPS operators, we can now understand what happens to the large  $N$  degeneracy at the two-loop level. According to Ref. [7], at one loop and in the large  $N$  limit all conformal invariants emerging in the pure HM projection coincide:

$$\mathcal{F}_\pm^{(k)}(s,t) = \mathcal{F}_m^{(k)}(s,t) = -\frac{\lambda}{N^2} \frac{k^2}{2} \Phi^{(1)}(s,t). \quad (2.21)$$

This degeneracy manifests itself already in the case  $k = 3$ : The single function,  $\mathcal{F}_+^{(3)}$ , describing the one-loop amplitude obeys the extra crossing symmetry relation  $\mathcal{F}_+^{(3)}(s, t) = \mathcal{F}_+^{(3)}(t, s)$  which is not required on general grounds. Just as in the one-loop case, the two-loop function  $\mathcal{F}_+^{(3)}$  from eq. (2.18) obeys eq. (2.17) imposed by the symmetry of the amplitude, but the one-loop “bonus” crossing symmetry relation does not hold anymore. We therefore conclude that this symmetry of the  $k = 3$  one-loop amplitude is destroyed by the two-loop quantum corrections.

Another type of degeneracy appears in the case  $k = 4$ . On the general grounds of superconformal and crossing symmetry two *a priori* independent conformal invariants are needed in this case, while at one loop both of them appear to coincide in the large  $N$  limit [7]. According to eqs. (2.18), at the two-loop level we indeed find two conformally invariant functions  $\mathcal{F}_\pm^{(4)}$  which are distinctly different. Again we observe that the one-loop degeneracy is lifted when the two-loop corrections are switched on.

However, we also see that both types of large  $N$  degeneracy mentioned above *still hold at the two-loop level for operators of higher weight,  $k > 4$* . Indeed, for  $k > 4$  the functions  $\mathcal{F}_m^{(k)}$  coincide (they are equal to  $\mathcal{F}_-^{(k)}$  for  $k$  odd) and have the same bonus crossing symmetry (2.17) as  $\mathcal{F}_-^{(k)}$ .

Finally, we mention that in the special case  $k = 2$  we find

$$\begin{aligned} \mathcal{F}^{(2)}(s, t) = & \frac{\lambda^2}{N^2} \left[ \frac{1}{4}(s+t+1)[\Phi^{(1)}(s, t)]^2 \right. \\ & \left. + \frac{1}{s}\Phi^{(2)}(t/s, 1/s) + \Phi^{(2)}(s, t) + \frac{1}{t}\Phi^{(2)}(s/t, 1/t) \right]. \end{aligned} \quad (2.22)$$

This result has been previously obtained in Refs. [18, 14].

### 3 Mixing and large $N$ degeneracy

In field theory  $\frac{1}{2}$ -BPS operators can be realized as mixtures of single- and multi-trace operators. Here we investigate whether the operator mixing can affect the degeneracy problem of four-point correlation functions. As an explicit example we consider the case of weight  $k = 4$  operators.

As discussed in Ref. [7], for  $\frac{1}{2}$ -BPS operators of weight  $k \leq 4$  the complete  $\mathcal{N} = 4$  four-point amplitude can be reconstructed from the “pure”  $\mathcal{N} = 2$  hypermultiplet projection, eq. (2.10). In particular, in the case  $k = 4$  we can write down

$$\langle Q^{(4)} \rangle = \sum_{m=0}^4 a_{m,4-m,0}^{(4)}(s, t) X^m Y^{4-m}. \quad (3.1)$$

This projection involves five of the fifteen coefficient functions of the original  $\mathcal{N} = 4$  amplitude, which belong to the three crossing equivalence classes  $(a_{040}^{(4)}, a_{400}^{(4)})$ ,  $(a_{130}^{(4)}, a_{310}^{(4)})$  and  $a_{220}^{(4)}$ .

In order to study possible mixing effects on  $Q^{(4)}$  we compute the coefficients  $a^{(4)}$  at tree level. There, generically, the  $\frac{1}{2}$ -BPS operator is of the form

$$\mathcal{O} \sim S + aD, \quad (3.2)$$

where we have defined

$$S \equiv \text{Tr}(q^4), \quad D \equiv \text{Tr}(q^2)\text{Tr}(q^2), \quad (3.3)$$

$q$  being the  $\mathcal{N} = 2$  Grassmann analytic HM superfield and  $a$  an  $N$ -dependent mixing parameter.

We fix the normalization coefficient for  $\mathcal{O}$  by requiring its two-point function to be normalized canonically. Computing separately the two-point functions  $\langle SS \rangle$ ,  $\langle SD \rangle$  and  $\langle DD \rangle$ , in the case of  $\text{SU}(N)$  color group we find (since we are interested in the color combinatorics we do not exhibit the space-time dependence of the correlators)

$$\begin{aligned} \langle SS \rangle &= 4(N^2 - 1) \mathcal{P}_1, \\ \langle SD \rangle &= 8(N^2 - 1) \mathcal{P}_2, \\ \langle DD \rangle &= 8(N^2 - 1) \mathcal{P}_3, \end{aligned} \quad (3.4)$$

where, for convenience, we have introduced

$$\mathcal{P}_1 = \frac{1}{N^2}(N^4 - 6N^2 + 18), \quad \mathcal{P}_2 = \frac{1}{N}(2N^2 - 3), \quad \mathcal{P}_3 = (N^2 + 1). \quad (3.5)$$

Therefore, the canonically normalized operator reads

$$\mathcal{O} = \left[ 4(N^2 - 1) (\mathcal{P}_1 + 4a\mathcal{P}_2 + 2a^2\mathcal{P}_3) \right]^{-\frac{1}{2}} (S + aD). \quad (3.6)$$

The tree level contributions to the coefficients  $a^{(4)}$  are given by diagrams with propagator structures as in Fig. 1, with  $l = 0$ ,  $n = 4 - m$ ,  $m = 0, \dots, 4$ . The coefficient functions  $a_{040}^{(4)}$  and  $a_{400}^{(4)}$  correspond to disconnected diagrams built as product of 2-point function diagrams. Therefore, given the above normalization, they are trivially equal to 1. In order to determine the other coefficients we need to compute the actual four-point amplitudes for the mixed operator  $\mathcal{O}$ . This can be achieved by evaluating separately the four-point functions  $\langle SSSS \rangle$ ,  $\langle DDDD \rangle$  and  $\langle SSSD \rangle$ ,  $\langle SSDD \rangle$ ,  $\langle SDDD \rangle$  as well as the amplitudes obtained from the latter by permuting  $S$  and  $D$ .

Since it is enough to compute one coefficient function within each crossing equivalence class, we concentrate, for instance, on the coefficient function  $a_{310}^{(4)}$ . It is convenient to first evaluate the building blocks of Fig. 2.

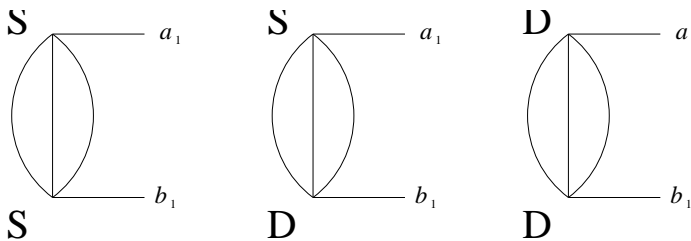


Figure 2. Building blocks for the coefficient  $a_{310}^{(4)}$ .

These building blocks can be obtained from the tree diagrams of the 2-point amplitudes (3.4) by cutting a line. This operation simply amounts to inserting a  $\delta_{a_1 b_1}$  for the line

cut without affecting the color structure. Therefore, the three building blocks are still proportional to the polynomials given in eq. (3.5). Explicitly,

$$\begin{aligned}
SS &\rightarrow 2^4 \mathcal{P}_1 \delta_{a_1 b_1} \\
SS &\rightarrow 2^5 \mathcal{P}_2 \delta_{a_1 b_1} \\
SS &\rightarrow 2^5 \mathcal{P}_3 \delta_{a_1 b_1}
\end{aligned} \tag{3.7}$$

These building blocks are then combined to realize all possible configurations of single- and double-trace operators. The result is

$$\begin{aligned}
a_{310}^{(4)} = a_{130}^{(4)} &= \frac{2^8 (N^2 - 1) (\mathcal{P}_1^2 + 16a^2 \mathcal{P}_2^2 + 4a^4 \mathcal{P}_3^2 + 8a \mathcal{P}_1 \mathcal{P}_2 + 16a^3 \mathcal{P}_2 \mathcal{P}_3 + 4a^2 \mathcal{P}_1 \mathcal{P}_3)}{2^4 (N^2 - 1)^2 (\mathcal{P}_1 + 4a \mathcal{P}_2 + 2a^2 \mathcal{P}_3)^2} \\
&= \frac{2^8 (N^2 - 1) (\mathcal{P}_1 + 4a \mathcal{P}_2 + 2a^2 \mathcal{P}_3)^2}{2^4 (N^2 - 1)^2 (\mathcal{P}_1 + 4a \mathcal{P}_2 + 2a^2 \mathcal{P}_3)^2} = \frac{16}{N^2 - 1},
\end{aligned} \tag{3.8}$$

Being independent of the mixing parameter  $a$ , it gives the finite  $N$  result for the tree level part of the coefficient function  $a_{310}^{(4)}$ , independently of the presence of the double-trace operator. In the large  $N$  limit this expression agrees with the result of Ref. [7]. We note that the independence of  $a$  is due to the particular structure (3.7) of the building blocks. For  $k \geq 4$  we observe the same phenomenon in the coefficients  $a_{(k-1)10}^{(k)}$ .

Next we concentrate on  $a_{220}^{(4)}$ . Again, the calculation can be carried out by first computing the building blocks depicted in Fig. 3.

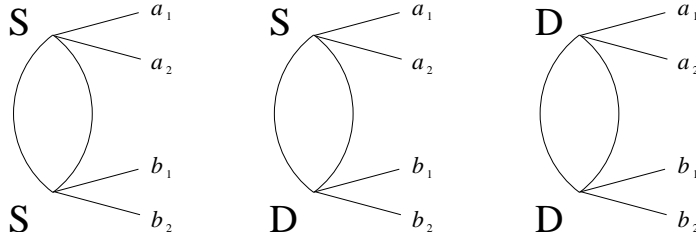


Figure 3. Building blocks for the coefficient  $a_{220}^{(4)}$ .

Introducing the concise notation  $\text{Tr}(T_a T_b \dots T_c T_d) \equiv (ab \dots cd)$  for the trace of the color generators, the algebraic expressions for the building blocks of Fig. 3 can be written as

$$\begin{aligned}
SS &\rightarrow 4 \frac{(N^2 - 9)}{N} [(a_1 a_2 b_1 b_2) + (a_2 a_1 b_1 b_2) + (a_1 a_2 b_2 b_1) + (a_2 a_1 b_2 b_1)] \\
&\quad + 8 \frac{2N^2 + 9}{N^2} (a_1 a_2)(b_1 b_2) + 4(a_1 b_1)(a_2 b_2) + 4(a_1 b_2)(a_2 b_1); \\
SD &\rightarrow 2^3 [(a_1 a_2 b_1 b_2) + (a_2 a_1 b_1 b_2) + (a_1 a_2 b_2 b_1) + (a_2 a_1 b_2 b_1) + (a_1 b_1 a_2 b_2) + (a_1 b_2 a_2 b_1)] \\
&\quad + \frac{(2N^2 - 3)}{N} (a_1 a_2)(b_1 b_2); \\
DD &\rightarrow 2^3 [(N^2 + 3)(a_1 a_2)(b_1 b_2) + 2(a_1 b_1)(a_2 b_2) + 2(a_1 b_2)(a_2 b_1)].
\end{aligned}$$

All possible configurations of the four-point amplitudes of  $S$  and  $D$  are obtained by combining the building blocks of Fig. 3 in all possible ways. The last contraction between two blocks produces an extra factor of 4. Pulling out the common factor  $2^8(N^2 - 1)$ , we find

$$\begin{aligned}
\langle SSSS \rangle &\rightarrow \left( N^4 - \frac{15}{2}N^2 + 135 - \frac{729}{N^2} + \frac{1215}{N^4} \right) \equiv \mathcal{P}_4, \\
\langle SSSD \rangle &\rightarrow \frac{1}{N^3}(10N^6 - 54N^4 + 216N^2 - 405) \equiv \mathcal{P}_5, \\
\langle SSDD \rangle &\rightarrow \frac{1}{N^2}(4N^6 + 6N^4 - 63N^2 + 135) \equiv \mathcal{P}_6, \\
\langle SDDD \rangle &\rightarrow \frac{1}{N}(2N^6 + 5N^4 + 18N^2 - 45) \equiv \mathcal{P}_7, \\
\langle DDDD \rangle &\rightarrow (N^6 + 5N^4 + 19N^2 + 15) \equiv \mathcal{P}_8
\end{aligned} \tag{3.9}$$

The final answer for the coefficient  $a_{220}^{(4)}$  is then

$$a_{220}^{(4)} = \frac{16(\mathcal{P}_4 + 4a\mathcal{P}_5 + 6a^2\mathcal{P}_6 + 4a^3\mathcal{P}_7 + a^4\mathcal{P}_8)}{(N^2 - 1)(\mathcal{P}_1 + 4a\mathcal{P}_2 + 2a^2\mathcal{P}_3)^2} \tag{3.10}$$

We notice that by setting  $a = 0$  (i.e., by neglecting the double-trace contributions) we obtain the finite  $N$  result for the free amplitude involving only the single-trace operator:

$$a_{220}^{(4) \text{ single}} = \frac{16(N^4 - \frac{15}{2}N^2 + 135 - \frac{729}{N^2} + \frac{1215}{N^4})}{(N^2 - 1)(N^2 - 6 + \frac{18}{N^2})^2} \tag{3.11}$$

In the large  $N$  limit this expression agrees with that in Ref. [7].

Next we analyze the large  $N$  limit of the general expression (3.10). Taking the large  $N$  limit of  $\mathcal{P}_i$  we obtain

$$a_{220}^{(4)} = \frac{16(N^2 + 40(Na) + 24(Na)^2 + 8(Na)^3 + (Na)^4)}{(N^2 + 8(Na) + 2(Na)^2)^2}. \tag{3.12}$$

If in the large  $N$  limit the mixing parameter is chosen to be of order one, then the double-trace part of  $\mathcal{O}$  provides a dominant contribution and one finds  $a_{220}^{(4)} \sim 1$ .

We recall that according to our general treatment in Section 2 the coefficient function  $a_{220}^{(4)}(s, t)$  admits a unique splitting on the non-trivial (“quantum”) function of the conformal cross-ratios constructed out of  $\mathcal{F}_\pm$  and an integration (“free field”) constant  $a_{220}^{(4)}$

$$a_{220}^{(4)}(s, t) = a_{220}^{(4)} + \mathcal{F}_+(s, t) + \mathcal{F}_+(1/s, t/s) + (t - s - 1)\mathcal{F}_-(t, s). \tag{3.13}$$

The constant part of  $a_{220}^{(4)}(s, t)$  was computed in the supergravity regime [7] with the result  $a_{220}^{(4) \text{ sugra}} = \frac{16}{N^2}$ , i.e. it scales as  $1/N^2$ . Therefore, the AdS/CFT correspondence does not allow the mixing parameter  $a$  to be of order one. If we pick  $a = \kappa/\sqrt{N} + \dots$ , then it will affect the coefficient  $a_{220}^{(4)}$  at order  $1/N^2$ :

$$a_{220}^{(4)} = \frac{16}{N^2}(1 + \kappa^4). \tag{3.14}$$

However, if we want  $a_{220}^{(4)}$  to match the large  $N$  value computed from supergravity exactly, we ought to require  $\kappa = 0$ , i.e. the mixing parameter has to scale faster than  $1/\sqrt{N}$ . Moreover, we note that if  $a$  is expanded in the odd powers of  $1/N$ , then the free amplitude has a 't Hooft type expansion in powers of  $1/N^2$ . Therefore, the simplest assumption for the mixing coefficient is  $a \sim 1/N + \dots$

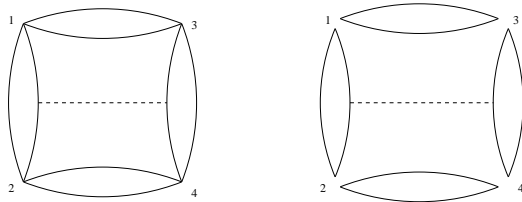


Figure 4. The leading large  $N$  contributions to the four-point amplitudes  $\langle SSSS \rangle$  and  $\langle DDDD \rangle$  at order  $\lambda$ .

Let us now briefly discuss the influence of the mixing on the large  $N$  degeneracy occurring at the one-loop level (order  $\lambda \equiv \frac{g^2}{4\pi}$ ). As shown in Ref. [7], harmonic analyticity, i.e. the superconformal kinematics, allows one to reduce the one-loop calculation of the four-point amplitude just to a single Feynman graph given in Fig. 4. This statement holds irrespectively of the intrinsic trace structure of the BPS operators and therefore it can be applied to the operator  $\mathcal{O}$ .

The various contributions to the coefficient  $a_{220}^{(4)}$  from the amplitude at order  $\lambda$  are then obtained by specifying the operator ( $S$  or  $D$ ) at each corner of the graph in Fig. 4. Using a double line notation for the propagators in there, the leading large  $N$  behavior is easily identified: Both the purely single-trace part  $\langle SSSS \rangle$  and the purely double-trace part  $\langle DDDD \rangle$  grow as  $N^7$ . This is in contradistinction to the free field case, where  $\langle SSSS \rangle \sim N^6$  while  $\langle DDDD \rangle \sim N^8$  (see eq. (3.9)). Therefore, at one loop the contribution of the double-trace operator appears to be more suppressed than in the free case, if compared to that of the single trace. The double-trace contribution can compete with the single-trace one if the mixing parameter is of order one. This is however ruled out by the free field considerations above which set  $a$  to scale faster than  $1/\sqrt{N}$ .

In conclusion, we see that if one requires the large  $N$  free field theory amplitude to coincide with the one for single-trace operators (and therefore with the constant part of the supergravity induced amplitude), then the mixing produces no effect on the leading large  $N$  one-loop amplitude and, as a consequence, on its degeneracy. Such a behavior follows the supergravity pattern: The redefinitions of the supergravity fields (corresponding to the field-theoretic mixing) produce no effect on the four-point amplitude, provided that it is of the regular (i.e., not of the extremal or sub-extremal) type [19].

## 4 The $\mathcal{N} = 2$ insertion procedure and Feynman rules

We would like to find the quantum corrections to the lowest component (at  $\theta_{1,2,3,4} = 0$ ) of the four-point correlator  $\langle Q^k \rangle$  and identify the corresponding conformal invariants  $\mathcal{F}$  in eq. (2.10). Already in the one-loop case, but even more so at two loops, the most

efficient technique, in our opinion, is the insertion procedure in  $\mathcal{N} = 2$  harmonic superspace [20, 17, 21, 22].

The basic ingredients of the  $\mathcal{N} = 4$  SYM theory in terms of  $\mathcal{N} = 2$  superfields are the hypermultiplet  $q^+(x, \theta^+, \bar{\theta}^+, u)$  and the  $\mathcal{N} = 2$  SYM field strength  $W(x, \theta)$ . The distinctive feature of the former is that it is a Grassmann analytic superfield (i.e., it depends only on the harmonic U(1) projections  $\theta^+, \bar{\theta}^+$ ) while the latter is a chiral superfield.

One of the advantages of the  $\mathcal{N} = 2$  formulation of the theory compared to  $\mathcal{N} = 1$  is that the HM composite operators like  $\text{Tr}(q^+)^k$  need no covariantization (no presence of the gauge superfield at the external points of the amplitude). Further, the HM matter interacts with the gauge sector only through a single cubic vertex. The true non-Abelian nature of the theory is encoded in the gauge self-interactions (as well as in the ghost sector, but we do not see it at the level  $g^4$ ).

The quantum corrections to the four-point correlator  $\langle Q^k \rangle$  at order  $g^4$  can be obtained by a double insertion of the  $\mathcal{N} = 2$  SYM action

$$S_{\mathcal{N}=2 \text{ SYM}} = \int d^4x d^4\theta \mathcal{L}, \quad \mathcal{L} = \frac{1}{4g^2} \text{Tr} W^2. \quad (4.1)$$

More precisely,

$$\langle Q^{(k)} \rangle_{g^4} = \frac{1}{2} \int d^4x_5 d^4\theta_5 d^4x_6 d^4\theta_6 \langle Q^{(k)} | \mathcal{L}(5) | \mathcal{L}(6) \rangle_{\text{tree}}. \quad (4.2)$$

Here  $\langle Q^{(k)} | \mathcal{L}(5) | \mathcal{L}(6) \rangle_{\text{tree}}$  is a new, six-point correlator calculated at “tree level” (Born approximation). The corresponding Feynman graphs are obtained by drawing the usual two-loop (order  $g^4$ ) graphs for  $\langle Q^{(k)} \rangle$  and then inserting the linearized  $\mathcal{N} = 2$  SYM Lagrangian  $\mathcal{L}$  into the gluon lines twice, each time into a different gluon line.<sup>7</sup>

The most important property of the new six-point amplitude is that it can be written in the factorized form

$$\langle Q^{(k)} | \mathcal{L} | \mathcal{L} \rangle = \Theta \times A^{(k-2)}(x, u), \quad (4.3)$$

where  $\Theta$  is a particular nilpotent six-point superconformal covariant carrying harmonic U(1) charge 2 at points 1 to 4, and R charge 2 at points 5 and 6 (the chiral field strength  $W$  has R charge 1 while the HMs carry harmonic U(1) but no R charge). Since the left-handed  $\theta_\alpha$  are the only superspace coordinates with positive R charge 1/2, we conclude that the expansion of  $\Theta$  must start with four such  $\theta$ s. The rest of the six-point correlator (4.3) is given by the function  $A^{(k-2)}(x, u)$  which carries U(1) charge  $k - 2$  at points 1 to 4 and can be expanded in the propagator basis as follows:

$$A^{(k-2)}(x, u) = \sum_{m=0}^{k-2} X^m Y^{k-m-2} A_m(x). \quad (4.4)$$

---

<sup>7</sup>This insertion procedure is based on the formula for the second derivative of the four-point correlator with respect to the gauge coupling constant:  $(\partial/\partial g^2)^2 \langle Q^{(k)} \rangle = \frac{2}{g^4} \int d^4x_5 d^4\theta_5 \langle Q^{(k)} | \mathcal{L} \rangle + \frac{1}{g^4} \int d^4x_5 d^4\theta_5 d^4x_6 d^4\theta_6 \langle Q^{(k)} | \mathcal{L} | \mathcal{L} \rangle$ . If both insertions are made into the same gluon line, this means inserting the chiral-to-chiral propagator  $\langle W(5)W(6) \rangle \sim \delta(5, 6)$  into that gluon line. By performing the chiral superspace integration over point 6, one can show that the five-point correlator arising in this way precisely cancels against the single-insertion term in this formula.

The coefficients  $A_m(x)$  are conformally covariant functions of the six space-time points. They have vanishing U(1) charge and are thus harmonic independent.

The structure of the nilpotent covariant  $\Theta$  is determined by superconformal symmetry combined with the Grassmann analytic (or  $\frac{1}{2}$ -BPS) nature of the first four points and the chiral nature of the last two points. The explicit form of  $\Theta$  (for  $\bar{\theta}_r^+ = 0$ ,  $r = 1, \dots, 4$ ) has been worked out in Ref. [22]:

$$\begin{aligned} \Theta &= \frac{\prod_{r=1}^4 x_{r5}^2 x_{r6}^2}{x_{56}^4} \frac{x_{12}^2 x_{34}^2 x_{13}^4 x_{24}^4}{R_{\mathcal{N}=2}} \\ &\times \left\{ [12]^2 [34]^2 \tau_{14} \tau_{23} + [14]^2 [23]^2 \tau_{12} \tau_{34} + [12][23][34][41] \left[ \tau_{13} \tau_{24} - \tau_{12} \tau_{34} - \tau_{14} \tau_{23} \right] \right\}. \end{aligned} \quad (4.5)$$

Here

$$\tau_{rs} \equiv 4(\rho_r \rho_s)(\sigma_r \sigma_s) + \rho_r^2 \sigma_s^2 + \rho_s^2 \sigma_r^2 \quad (4.6)$$

and

$$\rho_r = (\theta_r^+ - \theta_5^i u_{ri}^+) x_{r5}^{-1}, \quad \sigma_r = (\theta_r^+ - \theta_6^i u_{ri}^+) x_{r6}^{-1}, \quad r = 1, \dots, 4 \quad (4.7)$$

are Q-supersymmetry invariant combinations of the analytic  $\theta_r^+$  with the chiral  $\theta_{5,6}^i$  projected with the SU(2) harmonics  $(u_r)_i^+$ . The harmonic contractions [12], [34], etc. and the polynomial  $R_{\mathcal{N}=2}$  have been defined in eqs. (2.9) and (2.11), respectively.

The aim of our two-loop calculation is to determine the factor  $A^{(k-2)}(x, u)$  in the six-point covariant (4.3) and then to substitute everything in the insertion formula (4.2). Since we are only interested in the lowest component of the four-point correlator  $\langle Q^k \rangle$ , we can set all the external  $\theta$ s to zero,  $\theta_r^+ = \bar{\theta}_r^+ = 0$ ,  $r = 1, \dots, 4$ . In this case  $\Theta$  is rather simple:

$$\Theta_{\theta^+=0} = \theta_5^4 \theta_6^4 \frac{x_{12}^2 x_{34}^2 x_{13}^4 x_{24}^4}{x_{56}^4} R_{\mathcal{N}=2}. \quad (4.8)$$

Consequently, the six-point correlator becomes

$$\langle Q^{(k)} | \mathcal{L} | \mathcal{L} \rangle_{\theta^+=0} = \theta_5^4 \theta_6^4 \frac{x_{12}^2 x_{34}^2 x_{13}^4 x_{24}^4}{x_{56}^4} R_{\mathcal{N}=2} A^{(k-2)}(x, u). \quad (4.9)$$

Further, substituting this into the double-insertion formula (4.2) and performing the trivial chiral integrations over  $\theta_{5,6}$ , we obtain the two-loop correlator

$$\langle Q^{(k)} \rangle_{\theta^+=0} = x_{12}^2 x_{34}^2 x_{13}^4 x_{24}^4 R_{\mathcal{N}=2} \int \frac{d^4 x_5 d^4 x_6}{x_{56}^4} A^{(k-2)}(x, u). \quad (4.10)$$

Rewriting the amplitude in the form (2.10), we can read off the following expression for the conformally invariant coefficient functions  $\mathcal{F}^{(k)}$  at two loops:

$$\mathcal{F}_{m,k-m-2,0}^{(k)}(s, t) = x_{12}^2 x_{34}^2 x_{13}^4 x_{24}^4 \int \frac{d^4 x_5 d^4 x_6}{x_{56}^4} A_m(x). \quad (4.11)$$

Now, the practical question is how to compute  $A^{(k-2)}(x, u)$  (and hence  $A_m(x)$  and  $\mathcal{F}(s, t)$ ) from the corresponding set of two-loop Feynman diagrams. It turns out that instead of setting  $\theta^+ = 0$ , as required in the final expression (4.10), it is much more convenient to

do the computations with  $\theta_{5,6} = 0$ . The knowledge of the structure of  $\Theta$  (4.5) allows us to easily switch from one of these superconformal frames to the other.<sup>8</sup> In the new frame  $\Theta$  becomes even simpler,

$$\Theta_{\theta_{5,6}=0} = \prod_{r=1}^4 (\theta_r^+)^2, \quad (4.12)$$

so that eq. (4.9) is replaced by

$$\langle Q^{(k)} | \mathcal{L} | \mathcal{L} \rangle_{\theta_{5,6}=0} = \prod_{r=1}^4 (\theta_r^+)^2 A^{(k-2)}(x, u). \quad (4.13)$$

Then it is clear that in working out the expressions for the various Feynman graphs we can concentrate only on the terms with the maximal number of external  $\theta$ s. In particular, at order  $g^4$  this choice removes all graphs which contain non-Abelian interaction vertices. For example, the Y-shaped gluon subgraph in Fig. 5a vanishes because it has two chiral ends at the insertion points 5 and 6 and one analytic end (the gluon without insertion); after setting  $\theta_{5,6} = 0$  we are left with too few left-handed  $\theta$ s at the analytic gluon end to supply the required R charge 2. Similarly, the TTT block in Fig. 5a has three chiral ends (in fact, only two, points 6 and 7 should be identified) and two analytic ends; once again, the analytic  $\theta$ s cannot provide the required R charge 3.

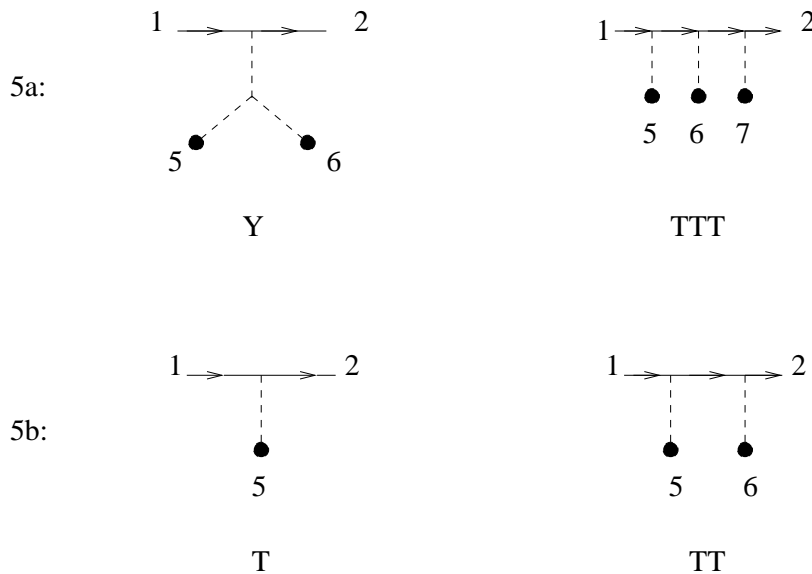


Figure 5. Building blocks of the Feynman graphs.

As a result of all these simplifications our task is reduced to listing all *tree level* Feynman graphs made out of the two building blocks T and TT in Fig. 5b. Although these blocks contain interaction vertices and hence integrals, the latter are easily computed using

<sup>8</sup>By “superconformal frames” we mean that  $\Theta$  can be cast into one of these forms by means of a finite superconformal transformations.

the harmonic superspace Feynman rules and they produce very simple *rational space-time functions* [20, 22]:

$$T_{125} \equiv \langle \tilde{q}^+(1)W(5)q^+(2) \rangle = \frac{2gf_{abc}}{(2\pi)^4 x_{12}^2} \left[ [21^-]\rho_1^2 + [12^-]\rho_2^2 - 2(\rho_1\rho_2) \right], \quad (4.14)$$

$$TT_{1562} \equiv \langle \tilde{q}^+(1)W(5)W(6)q^+(2) \rangle = -\frac{4g^2 f_{abc}f_{cde}}{(2\pi)^6 x_{12}^2} [1^-2^-]\rho_1^2 \sigma_2^2, \quad (4.15)$$

where  $\rho, \sigma$  have been defined in (4.7) and  $[12^-] = (u_1)_i^+ \epsilon^{ij} (u_2)_j^-$  (cf. (2.9)).

Notice the characteristic presence of negative-charged harmonics in both expressions (4.14) and (4.15). This has to do with the important issue of harmonic analyticity [15]. The point is that the free HM satisfies the massless field equation

$$D^{++}q^+(x, \theta^+, \bar{\theta}^+, u) = 0, \quad (4.16)$$

where

$$D^{++} = u^{+i} \frac{\partial}{\partial u^{-i}} - 4i\theta^+ \sigma^\mu \bar{\theta}^+ \frac{\partial}{\partial x^\mu} \quad (4.17)$$

is the supersymmetrized harmonic derivative (the raising operator of the group SU(2) realized on the charges  $\pm$  of the harmonics). This equation can also be viewed as a Cauchy-Riemann condition on the harmonic coset SU(2)/U(1), hence the name ‘‘harmonic analyticity’’. Yet another interpretation of eq. (4.16) is that it defines  $q^+$  as the highest weight state of an SU(2) irrep of charge 1 (isodoublet). When the HMs interact with the gauge sector, the harmonic derivative in (4.16) is modified by a gauge connection. Still, the gauge invariant composite operators like  $\text{Tr}(q^+)^k$  satisfy the same equation with a flat harmonic derivative. So, such operators correspond to the highest weight state of an SU(2) irrep of charge  $k$ .

As the simplest example of harmonic analyticity in action, consider the HM two-point function (propagator). It has to satisfy the Green’s function equation

$$D_1^{++} \langle \tilde{q}^+(1)q^+(2) \rangle = \delta(1, 2), \quad (4.18)$$

so here harmonic analyticity holds up to contact terms. The solution to this equation is (for simplicity we set  $\theta_2 = 0$ )

$$\langle \tilde{q}^+(1)q^+(2) \rangle = \frac{[12]}{\left( x_{12} + 4i \frac{[1^-2^-]}{[12]} \theta_1^+ \sigma \bar{\theta}_1^+ \right)^2}. \quad (4.19)$$

This can be checked by expanding the denominator in  $\theta_1^+ \bar{\theta}_1^+$ , using the relation  $\square_1(1/x_{12}^2) \sim \delta(x_{12})$  and the naive harmonic differentiation rules

$$D_1^{++} \theta_1^+ = 0, \quad D_1^{++} [1^-2^-] = [12], \quad D_1^{++} [12] = 0, \quad (4.20)$$

as well as the rule

$$D_1^{++} \frac{1}{[12]} = \delta(u_1, u_2) \quad (4.21)$$

which follows from the relation  $\partial/\partial \bar{z}(1/z) \sim \delta(z)$ . In the context of our four-point investigations we always set all  $\bar{\theta} = 0$ . Therefore here we never encounter harmonic singularities

of the type (4.21) and can safely apply the naive rules (4.20). Then harmonic analyticity simply means *polynomial dependence in  $u^+$  and no dependence in  $u^-$* . This is the case of the propagator (4.19) which now becomes

$$\langle \widehat{q}^+(1)q^+(2) \rangle_{\bar{\theta}=0} = \frac{[12]}{x_{12}^2}. \quad (4.22)$$

The same must hold for any  $n$ -point correlator of  $\frac{1}{2}$ -BPS operators: They must be polynomials in the harmonic variables  $u^+$  at each point.

Clearly, the expressions for the building blocks T (4.14) and TT (4.15) are not harmonic analytic because of the presence of  $1^-$  and  $2^-$ . This, however, is not a problem: The various building blocks or even complete Feynman graphs are not expected to be harmonic analytic, much like they are not conformal covariants. It is only the sum of all graphs that has these properties (see examples in Appendix A). In what follows we shall often profit from the expected harmonic analyticity of the final result to greatly simplify our graph calculations.

## 5 Two-loop four-point amplitudes

In this section we work in the frame  $\theta_{5,6} = 0$  where the six-point nilpotent covariant takes the form

$$\langle Q^{(k)} | \mathcal{L} | \mathcal{L} \rangle_{\theta_{5,6}=0} = \prod_{r=1}^4 (\theta_r^+)^2 \left[ \sum_{m=0}^{k-2} X^m Y^{k-m-2} A_m(x) \right]. \quad (5.1)$$

Here the coefficients  $A_m(x)$  are not all independent, as the crossing symmetry  $2 \leftrightarrow 3$  of eq. (2.10) implies that  $A_m(x)$  is equal to  $A_{k-m-2}(x)$  with  $x_2$  and  $x_3$  interchanged. In particular, for  $k$  even,  $A_{\frac{k-2}{2}}$  is invariant under this crossing transformation. By using eq. (4.11) one can see that these facts are in accord with the corresponding transformation property of  $\mathcal{F}_{m,k-m-2,0}^{(k)}(s,t)$ . Therefore, we need compute only  $(\frac{k-2}{2} + 1)$  coefficient functions if  $k$  is even and  $\frac{k-1}{2}$  if  $k$  is odd.

At two loops the correlator (5.1) is given by the sum of a number of Feynman graphs containing four interaction vertices of HM with gluons and two  $\mathcal{L}$  insertions. Let us discuss the general structure of these diagrams. According to the rules discussed in section 4, they are made out of the building blocks T and TT. The same argument based on  $\theta$  counting allows us to discard other sets of vanishing diagrams. Take, for instance, the graphs involving a HM loop with the insertion of two gluon lines connecting the HM propagators. Such a loop produces the expression  $(TT)^2 \sim \rho^4 \sigma^4 = 0$  (see (4.15)). For the same reason any graph containing a corner with all the incoming or outgoing HM lines being free vanishes, since this implies concentrating too many  $\theta$ s at some other corner. Finally, disconnected graphs containing subgraphs in the form of the one- or two-loop corrections to the two-point function of protected  $1/2$  BPS operators vanish as well.

With these rules in mind and observing that at order  $g^4$  the maximal number of HM lines involved in interactions with gluons is four, we can now draw all possible configurations. The planar interaction topologies *relevant* to the calculation of the functions  $A_m(x)$  are the same as the ones shown in Fig. 12 for the  $k = 4$  case (thin lines).<sup>9</sup> The complete graphs

<sup>9</sup>Beyond those of Fig. 12 there are also other interacting topologies which, however, play only an auxiliary rôle as it will become clear from our procedure of identifying the diagrammatic contributions to  $A_m(x)$ .

are then obtained by combining an interaction topology from Fig. 12 (thin lines) with the matching free HM frame from Fig. 6a. Each resulting topology is labeled by a pair of integers  $(p, q)$  ( $0 \leq p \leq 2m$ ,  $0 \leq q \leq 2(k - m - 2)$ ) which fixes the particular structure of the free HM lines. This procedure automatically takes into account the possible crossing symmetry transformations of the end points.

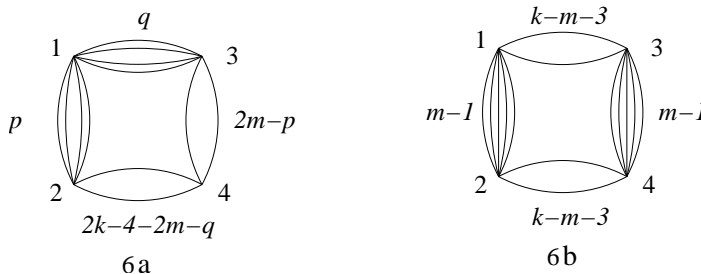


Figure 6. a) The free HM frame  $(p, q)$  associated with the function  $A_m(x)$ . b) The HM frame common to all graphs contributing to  $A_m(x)$ .

Evaluating the explicit expressions for each topology amounts to multiplying the building blocks (4.14) and (4.15) and using a simple Fierz identity for the two-component spinors  $\rho$  and  $\sigma$ . In this way the contributions of the individual graphs are always expressed in terms of the variables  $\rho_r^2$ ,  $\sigma_r^2$  and  $\tau_{rs}$ .

Since the building blocks contain negatively charged harmonic variables, each individual graph involves some non-analytic harmonic dependence. The final sum (5.1) must however be harmonic analytic and moreover, the coefficients  $A_m$  are harmonic independent. Thus, all the terms in the graphs with non-analytic dependence are in fact spurious and should cancel out. Due to the huge number of diagrams the evaluation of each diagram and the proof of the actual cancellation of non-analytic terms can be rather intricate (see Appendix A for a sample calculation).

However, the knowledge that the final result has to be analytic allows us to skip the actual computation of all the diagrams and directly identify a minimal set of graphs relevant to restoring the correct harmonic analytic structure of the final sum. This can be achieved by a suitable procedure of identifying the harmonics. In Appendix B we describe this procedure in detail when applied to operators of weight  $k = 3, 4$ . The corresponding minimal sets of relevant graphs for the  $k = 3$  case are given in Fig. 11, whereas for  $k = 4$  they are listed in Figs. 13 and 14.

For generic  $k$ , the procedure of identifying the harmonics goes along the same lines as in Appendix B. In this way, we are led to select the minimal set of relevant diagrams which contribute to the function  $A_m$ . They are drawn in Fig. 7 where the labels  $(p, q)$  are explicitly indicated for each graph.

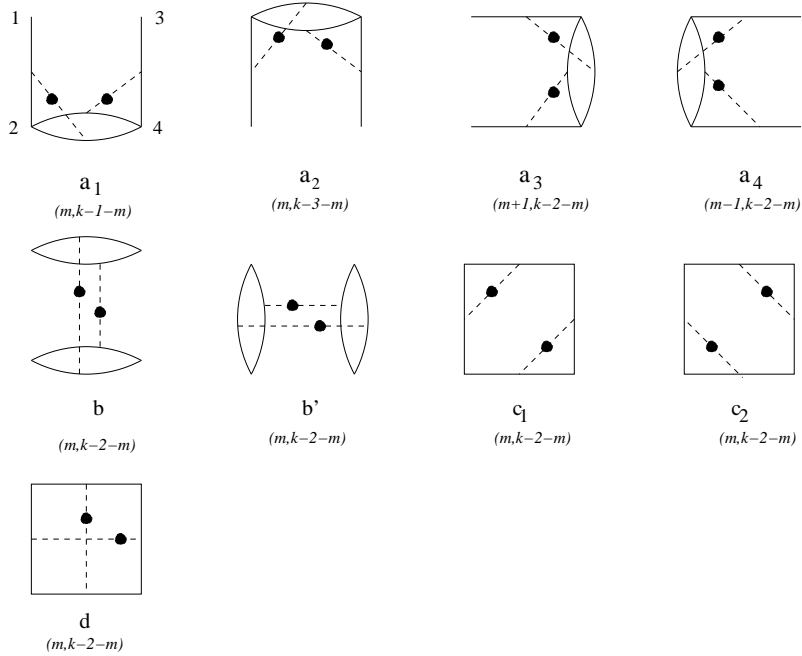


Figure 7. Relevant topologies of the interacting subgraphs of the planar graphs contributing to the function  $A_m$ . Every subgraph has to be multiplied by the free contribution from Fig. 6a.

We note that the topologies of interaction lines appearing in the diagrams of Fig. 7 are the same as the ones for  $k = 3, 4$  cases (see Figures 11–14 in Appendix B). Let us explain why this happens by first looking at the case  $1 \leq m \leq k - 3$ . We observe that the diagrams in Fig. 7 all contain the common free HM frame depicted in Fig. 6b. This frame provides the harmonic factor

$$X^{m-1}Y^{k-m-3} \rightarrow \left([12][43]\right)^{m-1} \left([13][42]\right)^{k-m-3} \quad (5.2)$$

which can be pulled out from all the graphs. It is easy to see that what remains forms the set of graphs contributing to the function  $A_1(x)$  for the amplitude of weight 4 operators (see Fig. 14). Therefore, we can exploit the results for  $k = 4$  to select the minimal set of interacting subdiagrams which survive harmonic identification. The particular cases  $m = 0$  and its crossing symmetry partner  $m = k - 2$  can be treated in the same way. For  $m = 0$  the graphs  $a_3$  and  $a_4$  in Fig. 7 are absent and pulling out a common factor  $Y^{k-4}$  we are led to the set of graphs for the function  $A_0$  of the  $k = 4$  case (see Fig. 13).

The important conclusion we reach at this point is that *the two-loop calculation for arbitrary  $k$  is reduced to that for  $k = 4$* . The reason for this is quite clear: Since at two loops at most four HM lines are involved in the interactions, for a sufficiently large  $k$  the majority of the HM lines play the rôle of “spectators”.

Let us explain why the diagrams in Fig. 7 with the labels  $(p, q)$  indicated do indeed provide the contributions to  $A_m$ . Recall that the graphs which contribute to  $A_m$  are the ones from which we can eventually extract the propagator factor  $X^m Y^{k-m-2}$ . We have already pulled out a common factor  $X^{m-1} Y^{k-m-3}$ . Leaving aside for the moment the

graphs of the type 7a we see that all the other diagrams contain an additional factor  $XY \sim [12][43][13][42]$ . Pulling it out we restore the required overall factor  $X^m Y^{k-m-2}$ . What remains from the graph is a chargeless combination of harmonics which may contain constant harmonic independent terms, but also non-analytic terms. However, once we have pulled out the required overall factor, the rest has to be harmonic independent and can be computed by identifying all the harmonics as explained in Appendix B.

We still have to take care of the graphs which contain interaction subgraphs of type 7a. For instance, for the interaction topology 7a<sub>1</sub> besides the common frame (5.2) we can also pull out an extra factor  $[12][43] \sim X$ . This leaves behind the free factor  $[13]^2$  which is different from the expected  $[13][42] \sim Y$ . The missing factor  $Y$  is restored only after summing up 7a<sub>1</sub> with all of its analyticity partners. The partners of the graph 7a<sub>1</sub> needed to restore analyticity, e.g., at points 1 and 3 are shown in Fig. 8. In Appendix A we analyze in detail how analyticity is achieved in this case and how such a long calculation can be efficiently bypassed by the procedure of identifying the harmonics.

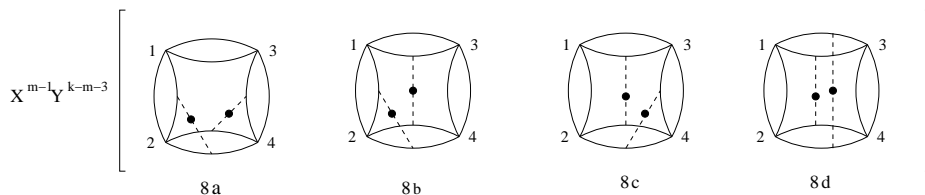


Figure 8. The graph 8a (topology 7a<sub>1</sub>) and its partners restoring analyticity at points 1 and 3 (all the graphs have the same bottom part). The common free HM frame has been pulled out as the prefactor  $X^{m-1} Y^{k-m-3}$ .

The reader may wonder why the graph 8d, which has the topology 7b, has been included in the set 8 where it clearly plays the auxiliary role of an analyticity partner of the graph 8a. In fact, this graph plays a dual role: It becomes the principal graph contributing to the coefficient function  $A_{m+1}(x)$ . Indeed, pulling out the common factor  $X^{m-1} Y^{k-m-3}$  and the extra factor  $X^2$  contained in the the graph 8d, we find

$$\left[ \tau_{13} - [13][1^- 3^-](\rho_1^2 \sigma_3^2 + \rho_3^2 \sigma_1^2) \right] \left[ \tau_{24} - [24][2^- 4^-](\rho_4^2 \sigma_2^2 + \rho_2^2 \sigma_4^2) \right]. \quad (5.3)$$

This expression is chargeless, so in it we can identify all the harmonics, after which we are left with the analytic term  $\tau_{13}\tau_{24}$ . We can say that the analytic part of eq. (5.3) contributes to the function  $A_{m+1}$ , while the non-analytic part combines with the other graphs in Fig. 8 into a harmonic analytic expression which gives a contribution to  $A_m$ .

Having identified the relevant graphs, we now proceed to computing the six-point cor-

relator. The Grassmann and space-time structures of the graphs in Fig. 7 are

$$\begin{aligned}
G_{a_1} &= \left( T_{125}T_{346} + (5 \leftrightarrow 6) \right) T_{245}T_{246} = \frac{\tau_{24}(\rho_1^2\sigma_3^2 + \rho_3^2\sigma_1^2)}{x_{24}^4 x_{12}^2 x_{34}^2}, \\
G_{a_2} &= \left( T_{125}T_{346} + (5 \leftrightarrow 6) \right) T_{135}T_{136} = \frac{\tau_{13}(\rho_2^2\sigma_4^2 + \rho_4^2\sigma_2^2)}{x_{13}^4 x_{12}^2 x_{34}^2}, \\
G_{a_3} &= \left( T_{135}T_{246} + (5 \leftrightarrow 6) \right) T_{345}T_{346} = \frac{\tau_{34}(\rho_1^2\sigma_2^2 + \rho_2^2\sigma_1^2)}{x_{13}^2 x_{24}^2 x_{34}^4}, \\
G_{a_4} &= \left( T_{135}T_{246} + (5 \leftrightarrow 6) \right) T_{125}T_{126} = \frac{\tau_{12}(\rho_3^2\sigma_4^2 + \rho_4^2\sigma_3^2)}{x_{12}^4 x_{13}^2 x_{24}^2}, \\
G_b &= T_{135}T_{136}T_{245}T_{246} + (5 \leftrightarrow 6) = 2 \frac{\tau_{13}\tau_{24}}{x_{13}^4 x_{24}^4}, \\
G_{b'} &= T_{125}T_{126}T_{345}T_{346} + (5 \leftrightarrow 6) = 2 \frac{\tau_{12}\tau_{34}}{x_{12}^4 x_{34}^4}, \\
G_{c_1} &= T_{125}T_{135}T_{246}T_{346} + (5 \leftrightarrow 6) = \frac{\tau_{23}(\rho_1^2\sigma_4^2 + \rho_4^2\sigma_1^2)}{x_{13}^2 x_{24}^2 x_{12}^2 x_{34}^2}, \\
G_{c_2} &= T_{125}T_{245}T_{136}T_{346} + (5 \leftrightarrow 6) = \frac{\tau_{14}(\rho_2^2\sigma_3^2 + \rho_3^2\sigma_2^2)}{x_{13}^2 x_{24}^2 x_{12}^2 x_{34}^2},
\end{aligned}$$

and

$$\begin{aligned}
G_d &= T_{125}T_{345}T_{136}T_{246} + (5 \leftrightarrow 6) \\
&= \frac{1}{x_{12}^2 x_{34}^2 x_{13}^2 x_{24}^2} \left[ \tau_{14}\tau_{23} - \tau_{13}\tau_{24} - \tau_{12}\tau_{34} - \tau_{23}(\rho_1^2\sigma_4^2 + \rho_4^2\sigma_1^2) - \tau_{14}(\rho_3^2\sigma_2^2 + \rho_2^2\sigma_3^2) \right. \\
&\quad \left. + \tau_{13}(\rho_4^2\sigma_2^2 + \rho_2^2\sigma_4^2) + \tau_{24}(\rho_1^2\sigma_3^2 + \rho_3^2\sigma_1^2) + \tau_{12}(\rho_4^2\sigma_3^2 + \rho_3^2\sigma_4^2) + \tau_{34}(\rho_1^2\sigma_2^2 + \rho_2^2\sigma_1^2) \right].
\end{aligned}$$

Collecting everything we arrive at the following complete harmonic analytic expression for the six-point correlator:

$$\begin{aligned}
\langle Q^{(k)} | \mathcal{L} | \mathcal{L} \rangle &\sim \frac{1}{x_{12}^2 x_{34}^2 x_{13}^2 x_{24}^2} \sum_{m=0}^{k-2} X^m Y^{k-m-2} \\
&\times \left\{ C_m^d \tau_{14} \tau_{23} + \left( 2s C_m^b - C_m^d \right) \tau_{13} \tau_{24} + \left( \frac{2}{s} C_m^{b'} - C_m^d \right) \tau_{12} \tau_{34} \right. \\
&\quad + (C_m^{c_1} - C_m^d) \tau_{23} (\rho_1^2 \sigma_4^2 + \rho_4^2 \sigma_1^2) + (C_m^{c_2} - C_m^d) \tau_{14} (\rho_3^2 \sigma_2^2 + \rho_2^2 \sigma_3^2) \\
&\quad + (C_m^d - C_m^{a_2}) \tau_{13} (\rho_4^2 \sigma_2^2 + \rho_2^2 \sigma_4^2) + (C_m^d - C_m^{a_1}) \tau_{24} (\rho_1^2 \sigma_3^2 + \rho_3^2 \sigma_1^2) \\
&\quad \left. + (C_m^d - C_m^{a_4}) \tau_{12} (\rho_4^2 \sigma_3^2 + \rho_3^2 \sigma_4^2) + (C_m^d - C_m^{a_3}) \tau_{34} (\rho_1^2 \sigma_2^2 + \rho_2^2 \sigma_1^2) \right\}.
\end{aligned} \tag{5.4}$$

where  $C_m$  denote the combinatorial factors associated to the various graphs.

The expression (5.4) has been derived for  $1 \leq m \leq k-3$ . As was already mentioned above, the cases  $m=0$  (and its crossing partner  $m=k-2$ ) are a bit special, as for  $m=0$  the graphs  $a_3$  and  $a_4$  are absent, while for  $m=k-2$  we do not have  $a_1$  and  $a_2$ . Otherwise, the derivation of the relevant contributions for these cases follows the same steps as above. Thus, the formula (5.4) remains valid for  $m=0$  and for  $m=k-2$  as well, provided we impose the following formal requirement on the combinatorial coefficients

$$C_0^{a_3} = C_0^{a_4} = C_{k-2}^{a_1} = C_{k-2}^{a_2} = 0.$$

Before we proceed, let us briefly discuss the general symmetry properties of the combinatorial factors. We note that for the graphs  $a_1$  and  $a_2$  the range of indices is  $0 \leq m \leq k-3$ , while for  $a_3$  and  $a_4$  it is  $1 \leq m \leq k-2$ . For a generic  $m$  the combinatorial coefficients  $C_m^{a_1}$  and  $C_m^{a_2}$  corresponding to the graphs  $a_1$  and  $a_2$  are equal,  $C_m^{a_1} = C_m^{a_2} \equiv C_m^a$  (though their analytic structures are different). Analogously,  $C_m^{a_3} = C_m^{a_4} \equiv C_m^{a'}$  and  $C_m^{c_1} = C_m^{c_2} = C_m^c$ . We also have the following additional relations

$$C_m^a = C_{k-m-2}^{a'}, \quad C_m^b = C_{k-m-2}^{b'}, \quad (5.5)$$

which in the special case  $m = m_-$  reduce to

$$C_{m_-}^a = C_{m_-}^{a'}, \quad C_{m_-}^b = C_{m_-}^{b'}. \quad (5.6)$$

Finally, to recast the six-point amplitude (5.4) in the form (5.1) we can use the relations

$$\rho_r^2 = \frac{\theta_r^{+2}}{x_{r5}^2}, \quad \sigma_r^2 = \frac{\theta_r^{+2}}{x_{r6}^2}, \quad \tau_{rs} = \theta_r^{+2} \theta_s^{+2} \frac{x_{rs}^2 x_{56}^2}{x_{r5}^2 x_{r6}^2 x_{s5}^2 x_{s6}^2} \quad (5.7)$$

valid for  $\theta_{5,6} = 0$ . The very last step is to perform the space-time integration over the insertion points 5 and 6 in eq. (4.11). This introduces the functions  $\Phi^{(1)}$  and  $\Phi^{(2)}$  defined in (2.19) and (2.20) and their point permutations. Note that  $\Phi^{(1)}$  is totally symmetric under permutations of the external points.

With these definitions at hand, from eqs. (5.1) and (4.11) we can identify

$$\begin{aligned} \mathcal{F}_{m,k-m-2,0}^{(k)}(s,t) = \varkappa & \left[ \frac{1}{4} \left( C_m^d t + (2C_m^b - C_m^d) s + (2C_m^{b'} - C_m^d) \right) [\Phi^{(1)}(s,t)]^2 \right. \\ & \left. + (C_m^d - C_m^{a'}) \frac{1}{s} \Phi^{(2)}(t/s, 1/s) + (C_m^d - C_m^a) \Phi^{(2)}(s,t) + (C_m^c - C_m^d) \frac{1}{t} \Phi^{(2)}(s/t, 1/t) \right]. \end{aligned} \quad (5.8)$$

Here  $\varkappa$  is an overall normalization coefficient independent of  $m$ , which is related to the normalization of the  $\frac{1}{2}$ -BPS operators.

The final result (5.8) essentially depends on the values of the combinatorial coefficients  $C_m$ . The particular crossing symmetry properties (2.17) of the functions  $\mathcal{F}_\pm$  provide some additional relations among the corresponding combinatorial coefficients. Indeed, for  $m = m_+$  we find

$$C_{m_+}^c = 2C_{m_+}^{b'} = 2C_{m_+}^d \quad (5.9)$$

but there are no new restrictions on  $C_{m_-}$ .

We remark that the case  $k = 2$  is special as there are no graphs of type 6a and the higher crossing symmetry requires  $2C_0^b = C_0^c = 2C_0^d$ .

The general expressions for the combinatorial coefficients  $C_m$  valid for finite  $N$  are

$$\begin{aligned}
C_m^a &= \frac{f_{qpe} f_{rte} f_{cse'} f_{nle'}}{2(m!)^2 (k-1-m)! (k-3-m)!} (a_1 \dots a_m a_{m+1} \dots a_{k-1} p) (a_1 \dots a_m b_{m+1} \dots b_{k-3} q r n) \\
&\times (c_1 \dots c_m a_{m+1} \dots a_{k-1} c) (c_1 \dots c_m b_{m+1} \dots b_{k-3} t s l), \\
2C_m^b &= \frac{f_{qpe} f_{rte} f_{cse'} f_{nle'}}{2[(k-m-2)! m!]^2} (a_1 \dots a_m a_{m+1} \dots a_{k-2} p s) (a_1 \dots a_m b_{m+1} \dots b_{k-2} r n) \\
&\times (c_1 \dots c_m a_{m+1} \dots a_{k-2} q c) (c_1 \dots c_m b_{m+1} \dots b_{k-2} t l), \\
C_m^c &= \frac{f_{qpe} f_{rte} f_{cse'} f_{nle'}}{2[(k-m-2)! m!]^2} (a_1 \dots a_m a_{m+1} \dots a_{k-2} p t) (a_1 \dots a_m b_{m+1} \dots b_{k-2} q n) \\
&\times (c_1 \dots c_m a_{m+1} \dots a_{k-2} r c) (c_1 \dots c_m b_{m+1} \dots b_{k-2} s l), \\
C_m^d &= \frac{f_{qpe} f_{rte} f_{cse'} f_{nle'}}{2[(k-m-2)! m!]^2} (a_1 \dots a_m a_{m+1} \dots a_{k-2} c p) (a_1 \dots a_m b_{m+1} \dots b_{k-2} l q) \\
&\times (c_1 \dots c_m a_{m+1} \dots a_{k-2} s r) (c_1 \dots c_m b_{m+1} \dots b_{k-2} n t),
\end{aligned}$$

where

$$(a_1 \dots a_k) \equiv \text{Tr} \left( t_{(a_1 \dots a_k)} \right)$$

is the symmetrized (without  $1/k!$ ) trace of  $k$  generators of the color group. In these formulae the combinatorial factors are necessary to prevent the overcounting of the HM lines induced by symmetrization.

To compute these coefficients in the large  $N$  limit we use the conventions  $[t_p, t_q] = i f_{p q e} t_e$  and  $f_{abe} f_{abe'} = 2N \delta_{ee'}$  as well as the following fusion and splitting rules

$$\begin{aligned}
(a_1 \dots a_l A) (a_1 \dots a_l B) &\approx (l+1)^2 l! N^{l-1} \text{Tr}(AB), \\
\text{Tr}[a_1 \dots a_l a_1 \dots a_l A] &\approx N^l \text{Tr} A.
\end{aligned}$$

In the large  $N$  limit we find

$$C_m^a = 2C_m^b = C_m^d = k^4 N^{2k}, \quad C_m^c = 2k^4 N^{2k}. \quad (5.10)$$

In this formula the range of the index  $m$  is  $0 \leq m \leq k-3$  for  $C_m^a$ ,  $0 \leq m \leq k-2$  for  $C_m^d$ ,  $1 \leq m \leq k-2$  for  $C_m^b$  and  $0 \leq m \leq k-2$  for  $C_m^c$ . The case of  $C_0^b$  deserves some special attention. Looking at the graph 6b for  $m=0$ , we realize that the gluon lines can “slide” along the HM loops, thus giving rise to two equivalent planar diagrams. Hence, the factor  $C_0^b$  is twice as big as the other  $C_m^b$  with  $m \neq 0$ :

$$C_0^b = k^4 N^{2k}. \quad (5.11)$$

So, the combinatorial coefficients have the remarkable property that they do not depend on  $m$ , except for the single “anomalous” coefficient  $C_m^b$  which changes its value only for  $m=0$ .

Substituting these combinatorial coefficients into eq. (5.8), choosing canonical normalization for the  $\frac{1}{2}$ -BPS operators and recalling the definition (2.16), we obtain our main result (2.18).

## 6 Two-loop four-point amplitudes from the OPE

Here we show that the four-point *two-loop amplitude* for  $\frac{1}{2}$ -BPS operators of weight 3 can be completely reconstructed just on the basis of the expected operator product expansion structure and the knowledge of the *one-loop anomalous dimensions* for certain operators of twist 2 and 4. Analogously, we obtain some restrictions on the structure of the amplitude for weight 4 operators. The discussion in this section provides an independent check on our diagrammatic computation.

### 6.1 Weight 3

The diagrammatic treatment clearly shows that at two loops the four-point amplitude is made out of two basic conformal integrals, (2.19) and (2.20). Therefore, the most general Ansatz compatible with the symmetry requirement  $\mathcal{F}(s, t) = 1/t \mathcal{F}(s/t, 1/t)$  is

$$\begin{aligned} \mathcal{F}(s, t) = & \frac{\lambda^2}{N^2} \cdot \left[ \frac{1}{4} (\varrho s + \eta(t+1)) [\Phi^{(1)}(s, t)]^2 \right. \\ & \left. + \frac{\mu}{s} \Phi^{(2)}(t/s, 1/s) + \nu \left( \Phi^{(2)}(s, t) + \frac{1}{t} \Phi^{(2)}(s/t, 1/t) \right) \right], \end{aligned} \quad (6.1)$$

i.e. each function depends on four unknown coefficients  $\varrho, \eta, \mu$  and  $\nu$ .

Already at the level of the free field theory one can see that the OPE  $\mathcal{O}^{(k)}\mathcal{O}^{(k)}$  of two  $\frac{1}{2}$ -BPS operators exhibits a heredity property: If some superconformal primary operator emerges in the spectrum of this OPE then it must also appear in the spectrum of  $\mathcal{O}^{(n)}\mathcal{O}^{(n)}$  with  $n > k$ . Therefore, knowing the spectrum of the operator product  $\mathcal{O}^{(2)}\mathcal{O}^{(2)}$  (see Refs. [25, 23]), we can use it to obtain restrictions on the four-point amplitude underlying the OPE of the  $\frac{1}{2}$ -BPS operators with higher weights. From the technical point of view, we need to build the conformal partial wave amplitude (CPWA) expansion of the conformal integrals entering eq. (6.1) and then to match the corresponding short-distance expansion of the four-point amplitude with perturbative CPWA contributions of operators with known anomalous dimensions. In this way one can fix the undetermined numerical coefficients in eq. (6.1).

The CPWA expansions of the conformal integrals in eq. (6.1), corresponding to taking a short-distance limit  $x_1 \rightarrow x_2, x_3 \rightarrow x_4$ , have already been obtained in Ref. [23] (cf. Section 3 there). They are formulated in terms of the conformal cross-ratios  $v = s/t$  and  $Y = (t-1)/t$ . Under the assumption that the conformal dimension  $\Delta$  of an operator is of the form  $\Delta = \Delta_0 + \gamma$ , where  $\Delta_0$  and  $\gamma$  are the canonical and the anomalous parts, respectively, the non-analytic term  $v^{\Delta/2}$  entering the CPWA of this operator gives rise to perturbative logarithms

$$v^{\Delta/2} = 1 + 1/2 \gamma \ln v + 1/8 \gamma^2 \ln^2 v + \dots$$

Therefore, the information about the one-loop (order  $\lambda$ ) anomalous dimensions is reflected in the coefficients of the  $\ln^2 v$  terms in the perturbative CPWA expansions and this is how we can use it to derive the form of the two-loop (order  $\lambda^2$ ) amplitude. The explicit calculations are not particularly instructive and therefore in the following we mainly restrict ourselves to the formulation of the results obtained.

*Operators of twist 2.*

The R-symmetry singlet of the OPE  $\mathcal{O}^{(2)}\mathcal{O}^{(2)}$  contains an infinite tower of twist 2 operators of increasing spin, the lowest member being the Konishi scalar of canonical dimension 2 and of one-loop anomalous dimension  $3\lambda$ . The requirement of reproducing this field in the OPE derived from eq. (6.1) fixes two of the four unknown coefficients, namely,

$$\eta = \nu = \frac{3^2}{4}. \quad (6.2)$$

Given relation (6.2), the whole tower of twist 2 operators is then correctly reproduced by the four-point amplitude. However, the operators of twist 2 produce no restrictions on the coefficients  $\varrho$  and  $\nu$ .

*Operators of twist 4 in the singlet channel.*

To get further restrictions on the four-point amplitude we consider the superconformal primary operators of twist 4 in the singlet R-symmetry channel. The simplest example are the four quadrilinear dimension 4 operators  $\Sigma_{1,2}, \Sigma_{\pm}$  studied in Ref. [24] (see also [5]). These operators diagonalize the matrix of the dilatation operator at one loop with the following result for the large  $N$  one-loop anomalous dimensions<sup>10</sup>

$$\gamma_1 = 0, \quad \gamma_2 = 6\lambda, \quad \gamma_{\Sigma_{\pm}} = \frac{1}{4}(13 \pm \sqrt{41})\lambda. \quad (6.3)$$

By using the explicit form of the (canonically normalized) operators  $\Sigma_{1,2}, \Sigma_{\pm}$  established in Ref. [24] we then compute their free three-point functions with the canonically normalized  $\frac{1}{2}$ -BPS operator  $\mathcal{O}^{(3)}$  in the large  $N$  limit and find

$$\sqrt{A_{\pm}} = \langle \mathcal{O}^{(3)}\mathcal{O}^{(3)}\Sigma_{\pm} \rangle = \frac{1}{N} \left( \frac{3}{5} \mp \frac{18}{5\sqrt{41}} \right)^{\frac{1}{2}}, \quad (6.4)$$

while  $\langle \mathcal{O}^{(3)}\mathcal{O}^{(3)}\Sigma_{1,2} \rangle \sim O(1/N^2)$ . Such a suppressed behavior of the three-point amplitudes involving  $\Sigma_{1,2}$  is naturally explained by the fact that these fields are double-trace operators. Thus, among the four operators only  $\Sigma_{\pm}$  participate in the large  $N$  operator product expansion of the four-point amplitude. The normalizations of their CPWAs are given by the constants  $A_{\pm}$ .

Combining the free, the one-loop amplitudes [7] and the two-loop Ansatz (6.1), we have worked out the corresponding CPWA expansion and have found the following system of equations<sup>11</sup> encoding the large  $N$  contribution of the fields  $\Sigma_{\pm}$ :

$$A_+ + A_- = \frac{6}{5N^2}, \quad (6.5)$$

$$A_+\gamma_{\Sigma_+} + A_-\gamma_{\Sigma_-} = \frac{21}{10} \frac{\lambda}{N^2}, \quad (6.6)$$

$$A_+\gamma_{\Sigma_+}^2 + A_-\gamma_{\Sigma_-}^2 = \left( \frac{81}{20} + \frac{8}{3}\varrho + \frac{4}{3}\mu \right) \frac{\lambda^2}{N^2}. \quad (6.7)$$

<sup>10</sup>At fixed  $\lambda$  the anomalous dimension  $\gamma_1$  vanishes only when  $N = \infty$  [24].

<sup>11</sup>These equations are obtained after careful disentangling of the contribution of the superconformal descendants of the twist 2 fields.

It is easy to check that the first two equations are indeed satisfied with the values of the  $A$ 's and  $\gamma$ 's found, while the third equation yields

$$\varrho = -\frac{\mu}{2}. \quad (6.8)$$

At this stage only one coefficient, e.g.  $\mu$ , remains undetermined.

*Operators of twist 4 in the irrep  $[0, 2, 0]$ .*

The OPE  $\mathcal{O}^{(2)}\mathcal{O}^{(2)}$  has ten different  $\text{SO}(6)$  channels. Among them only three may contain unprotected superconformal primary operators:  $[0, 0, 0]$ ,  $[0, 2, 0]$  and  $[1, 0, 1]$ . As we have already exploited the known information about the lowest dimensional operators in the singlet, now we move to the superconformal primaries of dimension 4 arising<sup>12</sup> in the irrep  $[0, 2, 0]$ .

There are four superconformal primary operators of canonical dimension 4 which might contribute to the operator product expansion under study. One of them is the protected semi-short double-trace operator [25]. The other three are long unprotected operators  $\Theta$ ,  $\Theta_{\pm}$  whose one-loop anomalous dimensions were found in Ref. [26] (see also [27]):

$$\gamma_{\Theta} = 3\lambda, \quad \gamma_{\Theta_{\pm}} = \frac{1}{2}(5 \pm \sqrt{5})\lambda. \quad (6.9)$$

The protected operator as well as  $\Theta$  are double-traces, therefore we do not expect them to contribute to the four-point amplitude in the large  $N$ -limit. Denoting by  $B_{\pm}$  the normalizations of the CPWAs of the operators  $\Theta_{\pm}$  and proceeding in the same manner as before, we find the following system of equations:

$$B_{+} + B_{-} = \frac{147}{4N^2}, \quad (6.10)$$

$$B_{+}\gamma_{\Theta_{+}} + B_{-}\gamma_{\Theta_{-}} = \frac{105\lambda}{2N^2}, \quad (6.11)$$

$$B_{+}\gamma_{\Theta_{+}}^2 + B_{-}\gamma_{\Theta_{-}}^2 = \frac{35\lambda^2}{4N^2}(9 + 2\mu). \quad (6.12)$$

The first two equations are used to find

$$B_{\pm} = \frac{21}{8N^2}(7 \mp 3\sqrt{5}). \quad (6.13)$$

The normalization constants are positive, as they should (the squares of the normalization coefficients of the three-point functions). Substituting these values in the third equation we find  $\mu = 0$ .

Thus, by exploiting the information about the one-loop anomalous dimensions of some superconformal primaries, we have completely determined the freedom in the most general Ansatz (6.1):

$$\varrho = \mu = 0, \quad \eta = \nu = \frac{3^2}{4}. \quad (6.14)$$

---

<sup>12</sup>There is only one  $\frac{1}{2}$ -BPS operator of dimension 2 in the irrep  $[0, 2, 0]$  and it does not produce any new restrictions on the four-point amplitude.

One can easily see that with these values the amplitude (6.1) indeed coincides with the function  $\mathcal{F}_+^{(3)}$  found in the previous section.

Finally, we remark that in Ref. [5] the two-loop anomalous dimensions for the operators  $\Theta_\pm$  were obtained

$$\gamma_\pm = -\frac{17 \pm 5\sqrt{5}}{8}\lambda^2. \quad (6.15)$$

Working out the logarithmic terms in the two-loop OPE implied by the four-point amplitude for  $k = 3$  we have checked that eq. (6.15) is indeed compatible with our findings provided the one-loop corrections to the normalization constants are

$$B_\pm = \langle \mathcal{O}^{(3)} \mathcal{O}^{(3)} \Theta_\pm \rangle^2 = \frac{21}{8N^2} (7 \mp 3\sqrt{5}) \left[ 1 - \frac{1}{20} (35 \pm 3\sqrt{5}) \lambda \right]. \quad (6.16)$$

## 6.2 Weight 4

Now we obtain some restrictions on the four-point two-loop amplitude for the  $\frac{1}{2}$ -BPS operators of weight 4 from the knowledge of the one-loop anomalous dimensions for the same operators of twist 2 and 4 that were already discussed in the previous section.

For  $k = 4$  we expect two functions  $\mathcal{F}_\pm^{(4)}$  with the symmetry property

$$\mathcal{F}_\pm^{(4)}(s, t) = 1/t \mathcal{F}_\pm^{(4)}(s/t, 1/t).$$

The general Ansätze compatible with these symmetries are

$$\begin{aligned} \mathcal{F}_\pm^{(4)}(s, t) &= \frac{\lambda^2}{N^2} \cdot \left[ \frac{1}{4} (\varrho_\pm s + \eta_\pm (t + 1)) [\Phi^{(1)}(s, t)]^2 \right. \\ &\quad \left. + \frac{\mu_\pm}{s} \Phi^{(2)}(t/s, 1/s) + \nu_\pm \left( \Phi^{(2)}(s, t) + \frac{1}{t} \Phi^{(2)}(s/t, 1/t) \right) \right], \end{aligned} \quad (6.17)$$

i.e. each function depends on four unknown coefficients  $\varrho, \eta, \mu$  and  $\nu$ .

*Operators of twist 2.*

This time the Konishi field (as well as its higher-spin cousins) imposes the following relations

$$\eta_+ = \nu_+ = \frac{4^2}{4} = 4, \quad (6.18)$$

while the other coefficients remain invisible. Clearly, these values of  $\eta_+, \nu_+$  coincide with those in eq. (2.18) obtained by explicit diagrammatic computations.

*Operators of twist 4 in the singlet channel.*

A calculation similar to the case  $k = 3$  produces the following system (after disentangling the contributions of the superconformal descendants of the twist 2 fields):

$$\begin{aligned} A_+ + A_- &= \frac{32}{15N^2}, \\ A_+ \gamma_{\Sigma_+} + A_- \gamma_{\Sigma_-} &= \frac{56}{15} \frac{\lambda}{N^2}, \\ A_+ \gamma_{\Sigma_+}^2 + A_- \gamma_{\Sigma_-}^2 &= \frac{2}{3} \left( 3\varrho_+ - \frac{6}{5} + \eta_- + 2\mu_- + 2\nu_- + \varrho_- \right) \frac{\lambda^2}{N^2}, \end{aligned} \quad (6.19)$$

where  $\gamma_{\Sigma_{\pm}}$  are given by eqs. (6.3). Solving this system we find

$$\eta_- = 12 - 3\rho_+ - 2\mu_- - 2\nu_- - \rho_- . \quad (6.20)$$

This completes our consideration of the singlet channel.

*Operators of twist 4 in the irrep  $[0, 2, 0]$ .*

The occurrence of the superconformal primaries  $\Theta_{\pm}$  in the double operator product expansion implied by the four-point amplitude leads to the following system of equations

$$\begin{aligned} B_+ + B_- &= \frac{2744}{25N^2} , \\ B_+\gamma_{\Theta_+} + B_-\gamma_{\Theta_-} &= \frac{784\lambda}{5N^2} , \\ B_+\gamma_{\Theta_+}^2 + B_-\gamma_{\Theta_-}^2 &= \frac{98\lambda^2}{5N^2}(\eta_- + 2\mu_- + 2\nu_- + \rho_-) . \end{aligned} \quad (6.21)$$

It allows us to find

$$\eta_- = 12 - 2\mu_- - 2\nu_- - \rho_- . \quad (6.22)$$

Comparing the last formula to eq. (6.20) gives  $\rho_+ = 0$ , which coincides with the corresponding value of the coefficient  $\rho_+$  in eq. (2.18).

This exhausts the predictive power of the method. The remaining coefficients  $\mu_{\pm}$ ,  $\nu_-$  and  $\rho_-$  can be found only from the diagrammatic computation. If we had the information about some other superconformal primaries appearing in the OPE for  $k = 3$  or  $k = 4$ , we could use it to further refine our Ansatz.

Finally, according to formula (2.18) we have

$$\mu_+ = \eta_- = \nu_- = 0 , \quad \mu_- = \rho_- = 4 . \quad (6.23)$$

With these values eq. (6.22) is trivially satisfied.

## Acknowledgements

We are grateful to N. Beisert, S. Frolov, S. Kovacs, H. Osborn, J. Plefka, Y. Stanev and M. Staudacher for many useful discussions. This work has been supported in part by INFN, MURST and the European Commission RTN program HPRN-CT-2000-00131, in which G. A. is associated to the University of Bonn, S. P. is associated to the University of Padova and A. S. is associated to the University of Torino. The work of G. A. has been also supported by RFBI grant N02-01-00695.

# Appendices

## A Harmonic analyticity constraints

In this Appendix we develop a set of systematic rules to select the relevant graphs contributing to a correlation function and find consistency conditions for the combinatorial coefficients. These rules are based on the general property of harmonic analyticity satisfied by any correlation function of composite operators in G-analytic harmonic superspace.

Harmonic analyticity for a composite operator  $\mathcal{O}^k = \text{Tr}(\tilde{q}^n q^{k-n})$  means  $D^{++}\mathcal{O}^k = 0$ , where  $D^{++}$  is the harmonic derivative given in (4.17). Correlation functions then satisfy

$$D_i^{++}\langle\mathcal{O}^k(1)\cdots\mathcal{O}^k(n)\rangle=0\quad i=1,\cdots,n\quad (\text{A.1})$$

(modulo contact terms). At every order in perturbation theory we can implement this condition directly on Feynman graphs. As a consequence of the identity

$$D_1^{++}\langle\tilde{q}^+(1)q^+(2)\rangle=-\langle\tilde{q}^+(1)q^+(2)\rangle\overleftarrow{D}_2^{++}=\delta(1,2)\quad (\text{A.2})$$

where  $\delta(1,2)$  is the delta function in the G-analytic harmonic superspace, every time the derivative hits a HM propagator shrinks it to a point. In particular, when  $D^{++}$  hits a free line we have a vanishing contribution (we neglect contact terms), whereas when it hits a HM line involved in an interaction with a gluon, the effect is to shrink the propagator line to a point and move the internal gluon vertex to coincide with an external vertex. A simple example is given in Fig. 9 where analyticity implemented at the vertex 1 of diagram  $a_1$  produces the shrunk configuration  $a_2$ .

If the same shrunk configuration can be obtained when hitting different graphs (but at the same point), we can say that all these graphs conspire together to restore harmonic analyticity at that point. Repeating this procedure, one eventually recovers the whole class of graphs needed to form a harmonic analytic amplitude.

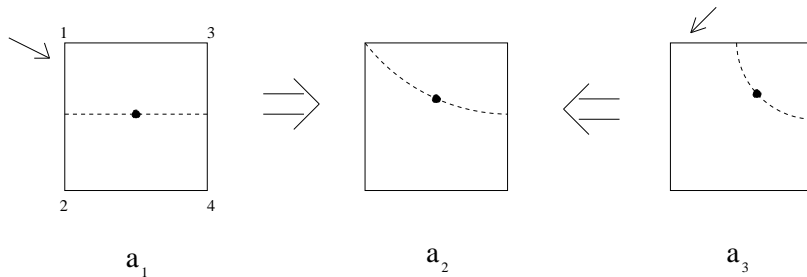


Figure 9. Example of an analyticity condition. The arrows point at the propagator hit by  $D_1^{++}$ .

Again, we exemplify this by taking the simple case of Fig. 9. There, the same shrunk configuration is obtained both from diagrams  $a_1$  and  $a_3$ . Since these are the only two diagrams which give the configuration  $a_2$  when hit at the point 1, the sum of their contributions

must result into an expression which is analytic in the 1 variable. In fact, using eq. (4.14) their contributions read

$$\begin{aligned} a_1 &\rightarrow C_{a_1} [13][42] \{ [21^-] \rho_1^2 + [12^-] \rho_2^2 - 2(\rho_1 \rho_2) \} \{ [43^-] \rho_3^2 + [34^-] \rho_4^2 - 2(\rho_3 \rho_4) \} \\ a_3 &\rightarrow C_{a_3} [12][42] \{ [31^-] \rho_1^2 + [13^-] \rho_3^2 - 2(\rho_1 \rho_3) \} \{ [43^-] \rho_3^2 + [34^-] \rho_4^2 - 2(\rho_3 \rho_4) \} \end{aligned} \quad (\text{A.3})$$

where  $C_{a_i}$  are the combinatorial factors (with possible signs included). The two expressions are non-analytic in the 1 variable because of their nontrivial dependence on  $u_1^-$ . The action of  $D_1^{++}$  on the sum of the two contributions must give zero, according to the condition (A.1). Remembering that  $D_1^{++}$  only acts on the  $u_1^-$  harmonic converting it into  $u_1^+$ , we obtain

$$(C_{a_1} + C_{a_3}) [42][13][21] \{ [43^-] \rho_1^2 \rho_3^2 + [34^-] \rho_1^2 \rho_4^2 \} = 0 \quad (\text{A.4})$$

which implies

$$C_{a_1} = -C_{a_3} \quad (\text{A.5})$$

Using this condition, the sum of the two contributions in (A.3) reads (we consider only the part depending on  $1^-$ )

$$[42] \{ [13][21^-] - [12][31^-] \} \{ [43^-] \rho_1^2 \rho_3^2 + [34^-] \rho_1^2 \rho_4^2 \} \quad (\text{A.6})$$

The harmonic cyclic identity

$$[13][21^-] - [12][31^-] = [23] \quad (\text{A.7})$$

shows that the non-analytic contributions from the two diagrams cancel against each other leaving an analytical result in the 1 variable.

As appears from this simple example, imposing analyticity conditions allows to draw systematically all the diagrams which at a given order contribute to the analytic final result for the correlation function and to find nontrivial relations like (A.5) which constrain the combinatorial coefficients. These relations can be used as a check when the coefficients are directly computed from the diagrams.

We notice that the final analytic result can be obtained by using a shortcut procedure: Given the sum of the two  $1^-$  dependent contributions in (A.3) we make the harmonics identification  $1 \equiv 2$ . As a consequence, the contribution from  $a_3$  vanishes whereas  $a_1$  gives

$$C_{a_1} [42][13][21^-] \{ [43^-] \rho_1^2 \rho_3^2 + [34^-] \rho_1^2 \rho_4^2 \} \stackrel{1 \equiv 2}{\implies} C_{a_1} [42][23] \{ [43^-] \rho_1^2 \rho_3^2 + [34^-] \rho_1^2 \rho_4^2 \} \quad (\text{A.8})$$

which is the correct result. The identification of the harmonics we chose is not the only possible one. We could have made the alternative identification  $1 \equiv 3$ . In this case the contribution from diagram  $a_1$  vanishes whereas from diagram  $a_3$  we obtain

$$C_{a_3} [12][42][31^-] \{ [43^-] \rho_1^2 \rho_3^2 + [34^-] \rho_1^2 \rho_4^2 \} \stackrel{1 \equiv 3}{\implies} -C_{a_3} [23][42] \{ [43^-] \rho_1^2 \rho_3^2 + [34^-] \rho_1^2 \rho_4^2 \} \quad (\text{A.9})$$

which again is the correct result.

We now consider the cases of our interest. We start by studying the analyticity conditions for the set of diagrams of Fig. 8 in the main text. They have in common two free lines which give the analytic structure  $[12][43]$  and a “base”  $T_{245}T_{246}$ :

$$\begin{aligned} T_{245}T_{246} &= [24^-][42^-](\rho_4^2\sigma_2^2 + \rho_2^2\sigma_4^2) + 4(\rho_2\rho_4)(\sigma_2\sigma_4) \\ &= \tau_{24} - [24][2^-4^-](\rho_4^2\sigma_2^2 + \rho_2^2\sigma_4^2). \end{aligned} \quad (\text{A.10})$$

It is easy to see that leaving aside the base as well as the free propagators leads to the following harmonic and Grassmann structures:

$$\begin{aligned} (8a) : \quad & [13]^2[T_{125}T_{436} + 5 \leftrightarrow 6] = [13]^2[21^-][43^-](\rho_1^2\sigma_3^2 + \rho_3^2\sigma_1^2) \\ (8b) : \quad & [13][43][T_{125}T_{136} + 5 \leftrightarrow 6] = [13][43][21^-][13^-](\rho_1^2\sigma_3^2 + \rho_3^2\sigma_1^2) \\ (8c) : \quad & [13][12][T_{435}T_{136} + 5 \leftrightarrow 6] = [13][12][43^-][31^-](\rho_1^2\sigma_3^2 + \rho_3^2\sigma_1^2) \\ (8d) : \quad & [12][43][T_{135}T_{136} + 5 \leftrightarrow 6] = 2[12][43] \{ -[13][1^-3^-](\rho_1^2\sigma_3^2 + \rho_3^2\sigma_1^2) + \tau_{13} \} \end{aligned} \quad (\text{A.11})$$

The factor 2 in the graph (8d) is due to the symmetrization  $5 \leftrightarrow 6$ . Note that this is the only graph from this set which gives an analytic contribution proportional to  $\tau_{13}$ . The other Grassmann term  $\rho_1^2\sigma_3^2 + \rho_3^2\sigma_1^2$  always appears with non-analytic harmonic factors. Collecting all such terms we find

$$[13] \{ C_a[12][43^-][31^-] + C_b[13][21^-][43^-] + C_c[43][21^-][13^-] - 2C_d[12][43][1^-3^-] \} \quad (\text{A.12})$$

where we have introduced combinatorial factors  $C_a, \dots, C_d$ . We want to achieve harmonic analyticity at points 1 and 3. According to the rule described above, we hit the graphs with harmonic derivatives  $D_1^{++}$  and  $D_3^{++}$ .

We begin by applying  $D_1^{++}$  to the expression (A.12) to obtain

$$[13][12] \{ (-C_b - 2C_d)[43][13^-] + (C_a + C_c)[43^-][31] \} = 0 \quad (\text{A.13})$$

Since the two harmonic structures within the brackets are linearly independent, we have the following two conditions

$$C_b = -2C_d \quad C_a = -C_c \quad (\text{A.14})$$

Similarly, hitting (A.12) with  $D_3^{++}$  we obtain

$$[13][43] \{ (C_a + C_b)[21^-][13] + (C_c + 2C_d)[12][31^-] \} = 0 \quad (\text{A.15})$$

which implies

$$C_c = -2C_d \quad C_a = -C_b \quad (\text{A.16})$$

The last set of conditions is consistent with (A.14) if  $C_b = C_c$ . This was somehow expected since graphs 8b) and 8c) only differ by a reflection ( $1 \leftrightarrow 3, 2 \leftrightarrow 4$ ) which should not affect the combinatorial factor.

We can solve the constraints (A.14) ending with only one arbitrary coefficient, e.g.  $C_d$ . With this choice for the coefficients the expression (A.12) becomes harmonic analytic with the help of the identity

$$[43][21^-][13^-] + [12][43^-][31^-] - [13][21^-][43^-] + [12][43][1^-3^-] = [42] \quad (\text{A.17})$$

Finally, taking all this into account, attaching the “base” and restoring the missing space-time factors, we find the total contribution of the graphs in Fig. 8 to be

$$\begin{aligned} \text{Total Fig. 8: } & \frac{2C_d[12][43]}{x_{12}^4 x_{13}^4 x_{24}^4 x_{34}^4} \{ -[13][42](\rho_1^2 \sigma_3^2 + \rho_3^2 \sigma_1^2) + [12][43]\tau_{13} \} \\ & \times \{ -[24][2^- 4^-](\rho_4^2 \sigma_2^2 + \rho_2^2 \sigma_4^2) + \tau_{24} \} \end{aligned} \quad (\text{A.18})$$

We see that analyticity at points 1 and 3 has indeed been achieved but not at points 2 and 4, of course.

As in the previous example, the correct result can be obtained by using harmonics identification. In fact, pulling out the free line contribution  $[12][43]$ , we can identify the harmonics  $1 \equiv 2$  and  $3 \equiv 4$ . As a consequence, in eq. (A.12) the contributions from diagrams a,c,d vanish and we are left with

$$C_b[13]^2[21^-][43^-](\rho_1^2 \sigma_3^2 + \rho_3^2 \sigma_1^2) \stackrel{1 \equiv 2, 3 \equiv 4}{\implies} C_b[13]^2(\rho_1^2 \sigma_3^2 + \rho_3^2 \sigma_1^2). \quad (\text{A.19})$$

Since the final result must be analytic, we can find an analytic term which under the above identification brings to the same expression

$$-C_b[13][42](\rho_1^2 \sigma_3^2 + \rho_3^2 \sigma_1^2) \stackrel{1 \equiv 2, 3 \equiv 4}{\implies} C_b[13]^2(\rho_1^2 \sigma_3^2 + \rho_3^2 \sigma_1^2). \quad (\text{A.20})$$

Therefore this must be the correct term which appears in the final result and it is indeed what we found in (A.18).

We notice that using this shortcut we can easily figure out the complete analytic structure for the sum of diagrams in fig. 8. In fact, analyticity at points 2 and 4, which should be restored by adding another set of partner graphs, can rather be obtained by identifying  $2 \equiv 4$ . This identification leaves the single term  $\tau_{24}$  in the bottom part of eq. (A.18) which becomes completely analytic.

We now consider the more complicated situation of graphs in Fig. 10. By imposing analyticity at points 1 and 4 we can find consistency conditions between the coefficients of the graphs 10c) which have been checked independently in Section 6, and the coefficients 10a) and 10b) which don't have any independent check. These conditions will necessarily involve new graphs contributing only to non-analytic structures, necessary in order to cancel similar terms coming from the graphs 10a), 10b) and 10c).

We start by considering the graph a) and apply the outlined procedure in order to achieve harmonic analyticity at points 1 and 4. It is easy to realize that in the large  $N$  limit, i.e. neglecting non-planar graphs, the set of conspiring graphs is just the one showed in Fig. 10.

As in the previous example, we write the harmonic and Grassmann factors coming from these graphs:

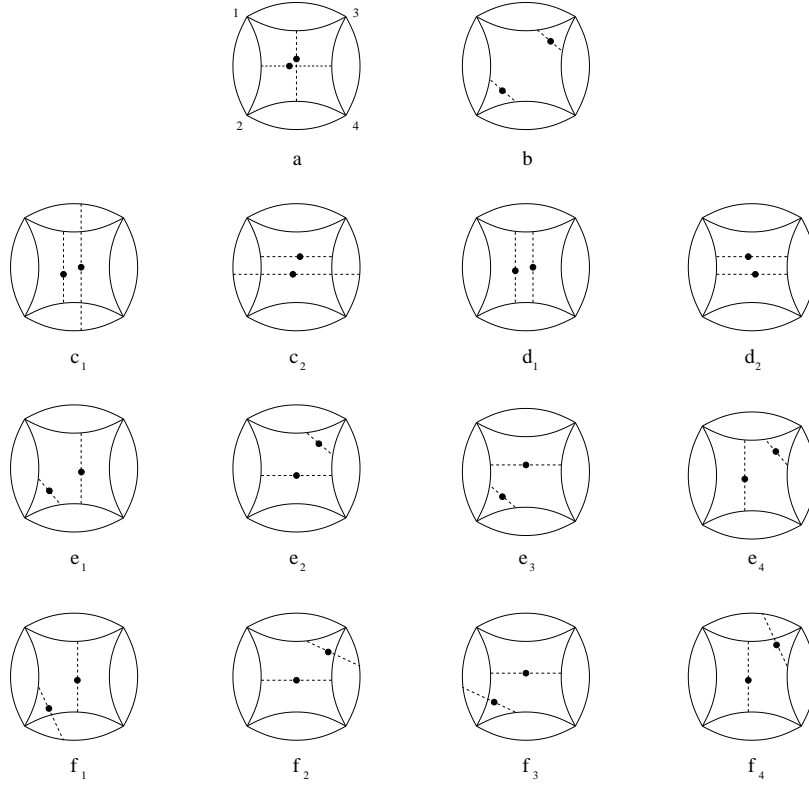


Figure 10. Graphs conspiring to harmonic analyticity at points 1 and 4.

$$\begin{aligned}
 (a) : \quad & [12][13][42][43][T_{135}T_{126}T_{425}T_{436} + 5 \leftrightarrow 6] \longrightarrow \\
 & [12][13][42][43] \left\{ [31^-][12^-][24^-][43^-] + [13^-][21^-][42^-][34^-] \right. \\
 & \quad \left. [\rho_1^2 \sigma_2^2 \sigma_3^2 \rho_4^2 + \sigma_1^2 \rho_2^2 \rho_3^2 \sigma_4^2] \right\}
 \end{aligned}$$

$$\begin{aligned}
 (b) : \quad & [12][13][42][43][T_{136}T_{125}T_{425}T_{436} + 5 \leftrightarrow 6] \longrightarrow \\
 & [12][13][42][43] \left\{ [31^-][12^-][24^-][43^-] [\rho_1^2 \sigma_2^2 \rho_3^2 \sigma_4^2 + \sigma_1^2 \rho_2^2 \sigma_3^2 \rho_4^2] \right. \\
 & \quad \left. + [13^-][21^-][42^-][34^-] [\sigma_1^2 \sigma_2^2 \rho_3^2 \rho_4^2 + \rho_1^2 \rho_2^2 \sigma_3^2 \sigma_4^2] \right\}
 \end{aligned}$$

$$\begin{aligned}
(c_1) : & \quad [12]^2[43]^2[T_{135}T_{136}T_{425}T_{426} + 5 \leftrightarrow 6] \longrightarrow \\
& \quad 2[12]^2[43]^2 \{ -[13][1^-3^-](\rho_1^2\sigma_3^2 + \rho_3^2\sigma_1^2) + \tau_{13} \} \{ -[24][2^-4^-](\rho_2^2\sigma_4^2 + \rho_4^2\sigma_2^2) + \tau_{24} \} \\
(c_2) : & \quad \text{same as } (c_1) \text{ with } 2 \leftrightarrow 3 \text{ or } 1 \leftrightarrow 4 \\
(d_1) : & \quad [12]^2[13][42][43]^2[(TT)_{1563}(TT)_{4652} + 5 \leftrightarrow 6] \longrightarrow \\
& \quad [12]^2[13][42][43]^2[1^-3^-][4^-2^-](\rho_1^2\rho_2^2\sigma_3^2\sigma_4^2 + \sigma_1^2\sigma_2^2\rho_3^2\rho_4^2) \\
(d_2) : & \quad \text{same as } (d_1) \text{ with } 2 \leftrightarrow 3 \text{ or } 1 \leftrightarrow 4 \\
(e_1) : & \quad [12][13][42][43]^2[T_{135}T_{126}(TT)_{4562} + 5 \leftrightarrow 6] \longrightarrow \\
& \quad [12][13][42][43]^2[2^-4^-][13^-][21^-](\sigma_1^2\sigma_2^2\rho_3^2\rho_4^2 + \rho_1^2\rho_2^2\sigma_3^2\sigma_4^2) \\
(e_2) : & \quad \text{same as } (e_1) \text{ with } 2 \leftrightarrow 3 \\
(e_3) : & \quad \text{same as } (e_1) \text{ with } 1 \leftrightarrow 4 \\
(e_4) : & \quad \text{same as } (e_1) \text{ with } 2 \leftrightarrow 3 \text{ and } 1 \leftrightarrow 4 \\
(f_1) : & \quad [12][13][43]^2[T_{135}T_{126}T_{425}T_{426} + 5 \leftrightarrow 6] \longrightarrow \\
& \quad [12][13][43]^2[13^-][21^-](\sigma_1^2\rho_3^2 + \rho_1^2\sigma_3^2) \{ -[24][2^-4^-](\rho_2^2\sigma_4^2 + \rho_4^2\sigma_2^2) + \tau_{24} \} \\
(f_2) : & \quad \text{same as } (f_1) \text{ with } 2 \leftrightarrow 3 \\
(f_3) : & \quad \text{same as } (f_1) \text{ with } 1 \leftrightarrow 4 \\
(f_4) : & \quad \text{same as } (f_1) \text{ with } 2 \leftrightarrow 3 \text{ and } 1 \leftrightarrow 4 \tag{A.21}
\end{aligned}$$

We concentrate on the contributions to the three independent structures not containing  $\tau$  factors

$$\begin{aligned}
U & \equiv \rho_1^2\rho_2^2\sigma_3^2\sigma_4^2 + \sigma_1^2\sigma_2^2\rho_3^2\rho_4^2 \\
V & \equiv \rho_1^2\sigma_2^2\rho_3^2\sigma_4^2 + \sigma_1^2\rho_2^2\sigma_3^2\rho_4^2 \\
Z & \equiv \rho_1^2\sigma_2^2\sigma_3^2\rho_4^2 + \sigma_1^2\rho_2^2\rho_3^2\sigma_4^2 \tag{A.22}
\end{aligned}$$

They are

$$\begin{aligned}
(a) : & \quad C_a[12][13][42][43] \left\{ [31^-][12^-][24^-][43^-] + [13^-][21^-][42^-][34^-] \right\} Z \\
(b) : & \quad C_b[12][13][42][43] \left\{ [31^-][12^-][24^-][43^-]V + [13^-][21^-][42^-][34^-]U \right\} \\
(c_1) : & \quad 2C_c[12]^2[43]^2[13][1^-3^-][24][2^-4^-](U + Z) \\
(c_2) : & \quad \text{same as } (c_1) \text{ with } 2 \leftrightarrow 3 \text{ or } 1 \leftrightarrow 4 \\
(d_1) : & \quad C_d[12]^2[13][42][43]^2[1^-3^-][4^-2^-]U \\
(d_2) : & \quad \text{same as } (d_1) \text{ with } 2 \leftrightarrow 3 \text{ or } 1 \leftrightarrow 4
\end{aligned}$$

$$\begin{aligned}
(e_1) : & C_e[12][13][42][43]^2[2^-4^-][13^-][21^-]U \\
(e_2) : & \text{same as } (e_1) \text{ with } 2 \leftrightarrow 3 \\
(e_3) : & \text{same as } (e_1) \text{ with } 1 \leftrightarrow 4 \\
(e_4) : & \text{same as } (e_1) \text{ with } 2 \leftrightarrow 3 \text{ and } 1 \leftrightarrow 4 \\
\\
(f_1) : & C_f[12][13][43]^2[13^-][21^-][42][2^-4^-](U + Z) \\
(f_2) : & \text{same as } (f_1) \text{ with } 2 \leftrightarrow 3 \\
(f_3) : & \text{same as } (f_1) \text{ with } 1 \leftrightarrow 4 \\
(f_4) : & \text{same as } (f_1) \text{ with } 2 \leftrightarrow 3 \text{ and } 1 \leftrightarrow 4
\end{aligned} \tag{A.23}$$

We have assumed that diagrams which differ by the exchange  $2 \leftrightarrow 3$  or/and  $1 \leftrightarrow 4$  have the same combinatorial factor.

By acting with  $D_1^{++}$  and setting to zero the independent structure proportional to  $U$  we get

$$\begin{aligned}
& [12][13][42][43] \left\{ [12][43][13^-][2^-4^-](-2C_c - C_d - C_e - C_f) \right. \\
& \quad \left. + [12][34^-][13^-][42^-](-C_b - C_e - C_f) \right\} = 0
\end{aligned} \tag{A.24}$$

Doing the same for the structure proportional to  $V$  gives an equation like (A.24) with  $2 \leftrightarrow 3$ , then it will not impose any new condition on the coefficients. The part proportional to  $Z$  gives instead

$$\begin{aligned}
& [12][13][42][43] \left\{ [12][43][13^-][2^-4^-](-2C_c - C_f) \right. \\
& \quad \left. + [12][34^-][13^-][42^-](-C_a - C_f) \right\} + 2 \leftrightarrow 3 = 0
\end{aligned} \tag{A.25}$$

By now setting to zero the two linearly independent analytic structure appearing in (A.24) and (A.25) we get the following conditions relating the coefficients of the graphs of Fig.10

$$\begin{aligned}
C_a &= 2C_c = -C_f \\
C_b &= C_a - C_e = C_a + C_d
\end{aligned} \tag{A.26}$$

We notice that the condition  $C_f = -2C_c$  has been already obtained in (A.16) (diagrams 10c) and 10f) are the same as 8d) and 8c), respectively).

It's now easy to see that there are no extra conditions coming from the terms containing one  $\tau$  factor. The same is true if we impose the analyticity condition at point 4. So we conclude that (A.26) is the full set of conditions imposed by the requirement of partial analyticity at points 1 and 4 on the graphs in Fig.10.

Using the relations (A.26) one can check that the total contribution obtained by summing the expressions in (A.21) ends up to be analytic in the 1 and 3 variables.

Again, as in the previous examples, the final answer can be obtained by suitable identification of the harmonics.

To summarize, what we have learned from the examples described above is the following: On one hand, imposing harmonic analyticity on the final result allows to find consistency conditions among the coefficients of different sets of graphs. On the other hand, once we give analyticity for granted, we can bypass the whole procedure of evaluating all diagrams conspiring to a final analytic result by performing harmonics identification, so drastically reducing the number of graphs to be computed.

## B Sample calculations: $k = 3$ and $k = 4$

In this Appendix we describe in detail the calculation of the  $A_m$  functions (see eq. (5.1)) for the cases  $k = 3$  and  $k = 4$ . In particular, we show how the procedure of identifying the harmonics can be used both to unambiguously select the diagrams which contribute to a given function and to drastically reduce the number of diagrams one needs compute.

### B.1 The case $k = 3$

The expected form of the complete amplitude for  $k = 3$  case is:

$$\langle Q^{(3)} | \mathcal{L} | \mathcal{L} \rangle_{\theta_{5,6}=0} \sim \prod_{r=1}^4 (\theta_r^+)^2 \left[ \frac{[13][42]}{x_{13}^2 x_{42}^2} A_0(x) + \frac{[12][43]}{x_{12}^2 x_{43}^2} A_1(x) \right] \quad (\text{B.1})$$

As discussed in the main text, the two functions  $A_0, A_1$  are related by crossing symmetry, and we need compute only one of them. To calculate for example  $A_0$ , it is sufficient to look at contributions proportional to the harmonic structure  $[13][42]$  in (B.1). They can be unambiguously selected by identifying the harmonics  $1 \equiv 2$  and  $3 \equiv 4$  in (B.1)

$$\langle Q^{(3)} | \mathcal{L} | \mathcal{L} \rangle_{\theta_{5,6}=0} \sim \prod_{r=1}^4 (\theta_r^+)^2 \left[ \frac{[13]^2}{x_{13}^2 x_{42}^2} A_0(x) \right] \quad (\text{B.2})$$

When looking at perturbative contributions at two loops, the harmonics identification implies the vanishing of all graphs containing:

- (i) at least one free line  $1 \rightarrow 2$  or  $3 \leftarrow 4$
- (ii) the blocks  $TT_{1562}$  or  $TT_{3564}$
- (iii) the blocks  $T_{125}T_{125}$  and alike

Discarding also the graphs which vanish by simple theta counting (see the general discussion in Sect. 5), the relevant surviving diagrams are then shown in Fig. 11. Upon the above harmonic identification, they already contain the analytic factor  $[13]^2$  required in eq. (B.2). Since the coefficient function  $A_0$  is independent of the harmonics, once we have pulled  $[13]^2$  out, we can go a step further and identify the harmonics  $1 \equiv 3$  in the rest of the expression.

As a consequence, the contributions from graphs 11c and 11d drop out. In the rest the harmonic dependence reduces to a common factor and, neglecting the space-time structure, the final contribution of each diagram is given by its combinatorics

$$\begin{aligned} 2C_a^{(11)} &= 2 \times 3^4 N^6 \\ C_b^{(11)} &= C_e^{(11)} = C_f^{(11)} = 3^4 N^6 \\ C_{g_1}^{(11)} &= C_{g_2}^{(11)} = 2 \times 3^4 N^6 \\ 2C_h^{(11)} &= 3^4 N^6 \end{aligned} \quad (\text{B.3})$$

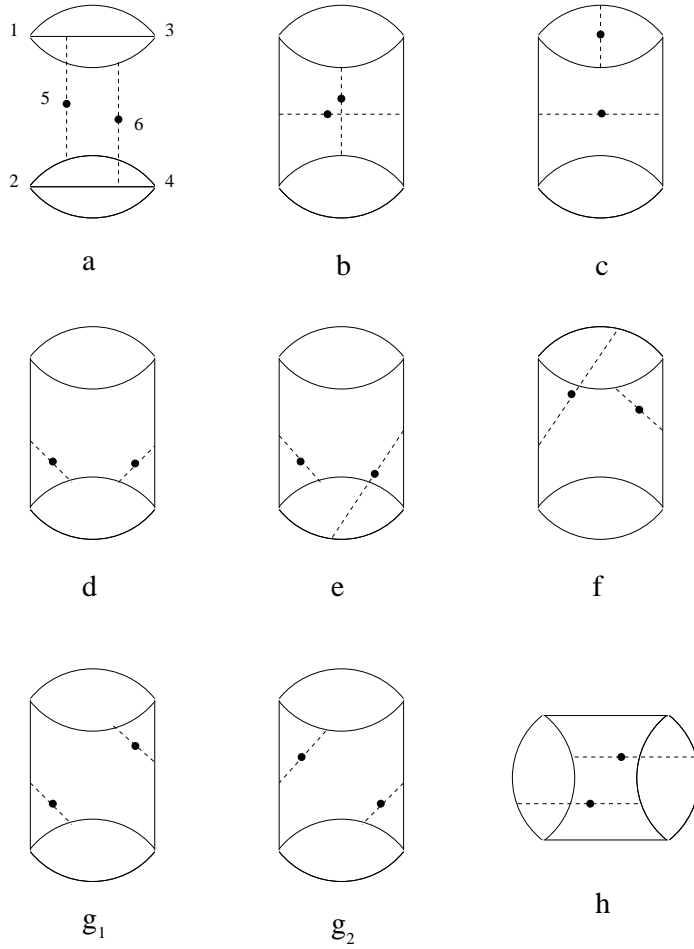


Figure 11. Relevant graphs for the  $k = 3$  case.

The extra factor 2 in front of  $C_a^{(11)}$  and  $C_h^{(11)}$  is due to the symmetry of the corresponding diagrams under the exchange  $5 \leftrightarrow 6$ .

In this simple example it is already clear how one can exploit the condition of harmonic analyticity of the final result. It is in fact this condition which allowed us to make the identification  $1 \equiv 3$ , thus reducing the number of Feynman diagrams to be computed. In a complete calculation performed without identifying the harmonics, the diagrams which vanished under this identification would contribute only to cancel non-analytic terms coming from the rest of the diagrams.

## B.2 The case $k = 4$

We now consider the more complicated case  $k = 4$ . There we have

$$\begin{aligned} \langle Q^{(4)} | \mathcal{L} | \mathcal{L} \rangle_{\theta_{5,6}=0} &\sim \prod_{r=1}^4 (\theta_r^+)^2 \\ &\times \left[ \left( \frac{[13][42]}{x_{13}^2 x_{42}^2} \right)^2 A_0(x) + \left( \frac{[13][42]}{x_{13}^2 x_{42}^2} \frac{[12][43]}{x_{12}^2 x_{43}^2} \right) A_1(x) + \left( \frac{[12][43]}{x_{12}^2 x_{43}^2} \right)^2 A_2(x) \right]. \end{aligned} \quad (\text{B.4})$$

This correlator is crossing symmetric under the exchange  $2 \leftrightarrow 3$  which relates the coefficient functions  $A_0$  and  $A_2$  to each other, while  $A_1$  is crossing symmetric and independent. Therefore, we need to perform the calculation in two independent channels.

To select the relevant graphs which contribute in the two channels we observe that in the  $k = 4$  case we have 8 HM lines and 2 gluons, which can at most connect 4 HM lines. Therefore, at least 4 HM lines remain free. If these free lines form a free corner, i.e. they all come out from the same vertex, we know that such graphs vanish because of theta counting (see the general discussion in sect. 5). It follows that the free lines have to form at least one disconnected pair.

If the free pair is  $[13][42]$ , such graphs can contribute to the functions  $A_0, A_1$  in eq. (B.4) but not to  $A_2$ . Then we can write down the contribution of all such graphs with a free pair  $[13][42]$  in the form

$$\frac{[13][42]}{x_{13}^2 x_{42}^2} \left[ \frac{[13][42]}{x_{13}^2 x_{42}^2} A_0(x) + \frac{[12][43]}{x_{12}^2 x_{43}^2} A_1(x) \right] \quad (\text{B.5})$$

Pulling out the factor  $\frac{[13][42]}{x_{13}^2 x_{42}^2}$  is equivalent to removing the corresponding free lines from the graphs, which results in a configuration with  $k = 3$ . Then we can go a step further and identify the harmonics pairwise within the brackets. If we identify  $1 \equiv 2, 3 \equiv 4$  and the graph does not vanish, then it contributes to  $A_0$ . If instead we identify  $1 \equiv 3, 2 \equiv 4$  and the graph does not vanish, then it contributes to  $A_1$ . Note that it may happen that the graph vanishes under each of these identifications, then it should be discarded.

Alternatively, if the free pair is  $[12][34]$ , eq. (B.5) is replaced by

$$\frac{[12][43]}{x_{12}^2 x_{43}^2} \left[ \frac{[13][42]}{x_{13}^2 x_{42}^2} A_1(x) + \frac{[12][43]}{x_{12}^2 x_{43}^2} A_2(x) \right] \quad (\text{B.6})$$

Once again, removing the free lines we obtain a  $k = 3$  configuration in which we identify the harmonics pairwise within the brackets. If we identify  $1 \equiv 2, 3 \equiv 4$  and the graph does not vanish, then it contributes to  $A_1$ . If instead we identify  $1 \equiv 3, 2 \equiv 4$  and the graph does not vanish, then it contributes to  $A_2$ .

We now use this strategy to select the relevant diagrams which eventually contribute to the coefficient functions. We carefully draw all the diagrams which are nonvanishing for theta counting and select the ones which survive under one of the harmonics identifications described above. We are then led to the set of graphs on Fig. 12 where, in order to reduce the number of diagrams, we have indicated with thick lines all free HM propagators, whereas thin lines are interacting (they contain an interaction vertex and gluons connect these vertices in all possible ways). All the graphs have 4 free lines and they have been organized according to the number of free lines coming out of a single point. We have

not drawn those diagrams that vanish after harmonics identification (the analog of graphs 11c and 11d of the previous example). As already explained, in an exhaustive calculation done without identifying harmonics these diagrams would conspire to cancel nonanalytic contributions from the rest.

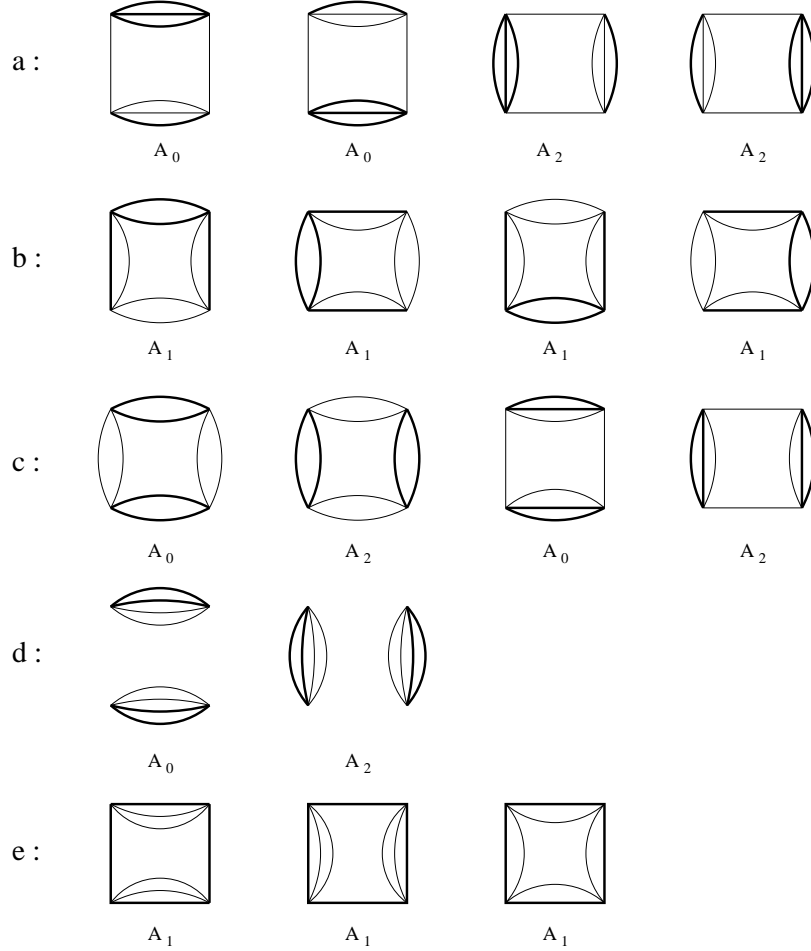


Figure 12. Relevant graphs for  $k = 4$ . The thick lines are free HM propagators whereas thin lines contain vertices of interaction with gluons.

We now apply the harmonics identification procedure to figure out which diagrams contribute to which function. Let us analyze in detail the graphs in Fig 12a. The first kind of graphs contain a free pair [13][42], so they belong to the type of eq. (B.5). According to the rule above, we pull out the free factor and then we identify the harmonics pairwise. The identification  $1 \equiv 3$ ,  $2 \equiv 4$  annihilates the graphs, so they cannot contribute to  $A_1$ . On the contrary, the graphs can survive the identification  $1 \equiv 2$ ,  $3 \equiv 4$ , so they contribute to  $A_0$ . If we now draw the gluons, we see that only one configuration is allowed and the graph is reduced to 11e from the case  $k = 3$ . The same argument applies to the second kind of graphs 12a, reducing them to a single structure like 11f. Similarly, the third and the fourth graphs 12a contain a free pair [12][43], so they belong to the type of eq. (B.6). According

to the rule above, we pull out the free factor and then we identify the harmonics pairwise. The identification  $1 \equiv 2, 3 \equiv 4$  annihilates the graphs, so they cannot contribute to  $A_1$ . On the contrary, the graphs survive the identification  $1 \equiv 3, 2 \equiv 4$ , so they contribute to  $A_2$ . If we now draw the gluons, we see that these graphs are reduced to 11e, 11f rotated by  $90^\circ$ .

Analyzing all the graphs along the same lines we eventually identify the coefficient functions they contribute to. The complete identification is indicated in Fig. 12. Drawing the gluon lines brings us to the diagrams in Fig. 13 for  $A_0$  and Fig. 14 for  $A_1$ .

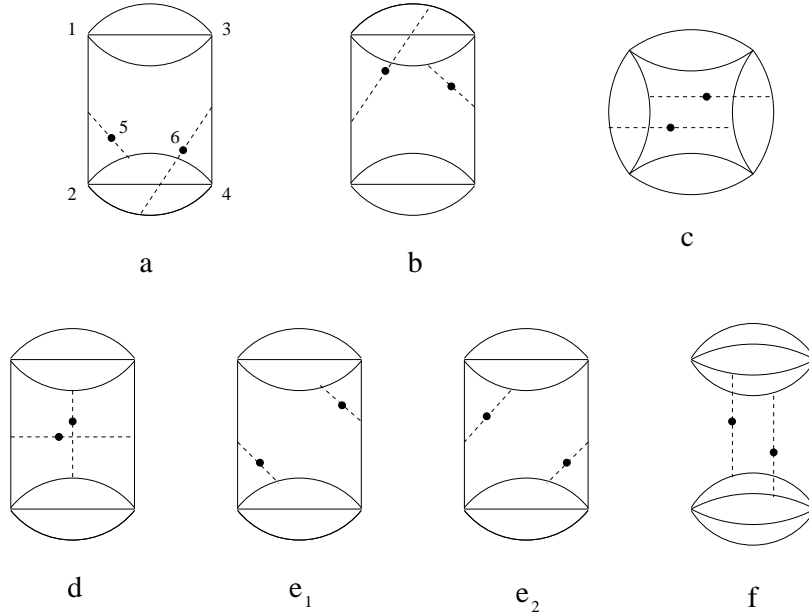


Figure 13. Diagrams contributing to the  $A_0$  function for  $k = 4$  case.

A couple of comments are now in order. First of all we notice that the configurations of gluon lines appearing in Figs.13 and 14 are the same as the ones we have already selected for  $k = 3$ . Moreover, a diagram with a given configuration of interacting lines can contribute to different functions according to the structure of free propagators which dress it. In fact, all the allowed configurations of interacting lines are present for both functions.

Now, computing the contribution of each graph is simply a matter of combinatorics. At large  $N$ , neglecting the space-time structure, for the  $A_0$  function we obtain

$$\begin{aligned}
 C_a^{(13)} &= C_b^{(13)} = 4^4 N^8 \\
 2C_c^{(13)} &= 4^4 N^8 \\
 C_d^{(13)} &= 4^4 N^8 \\
 C_{e_1}^{(13)} &= C_{e_2}^{(13)} = 2 \times 4^4 N^8 \\
 2C_f^{(13)} &= 2 \times 4^4 N^8
 \end{aligned} \tag{B.7}$$

whereas for  $A_1$

$$\begin{aligned}
 C_a^{(14)} &= C_b^{(14)} = C_c^{(14)} = C_d^{(14)} = 4^4 N^8 \\
 2C_e^{(14)} &= 4^4 N^8 \\
 2C_f^{(14)} &= 4^4 N^8 \\
 C_g^{(14)} &= 4^4 N^8 \\
 C_{h_1}^{(14)} &= C_{h_2}^{(14)} = 2 \times 4^4 N^8
 \end{aligned}
 \tag{B.8}$$

It is important to notice that, at large  $N$ , the combinatorial factors only depend on the structure of the interacting lines: Diagrams with the same interactions but different configurations of free propagators have the same coefficient.

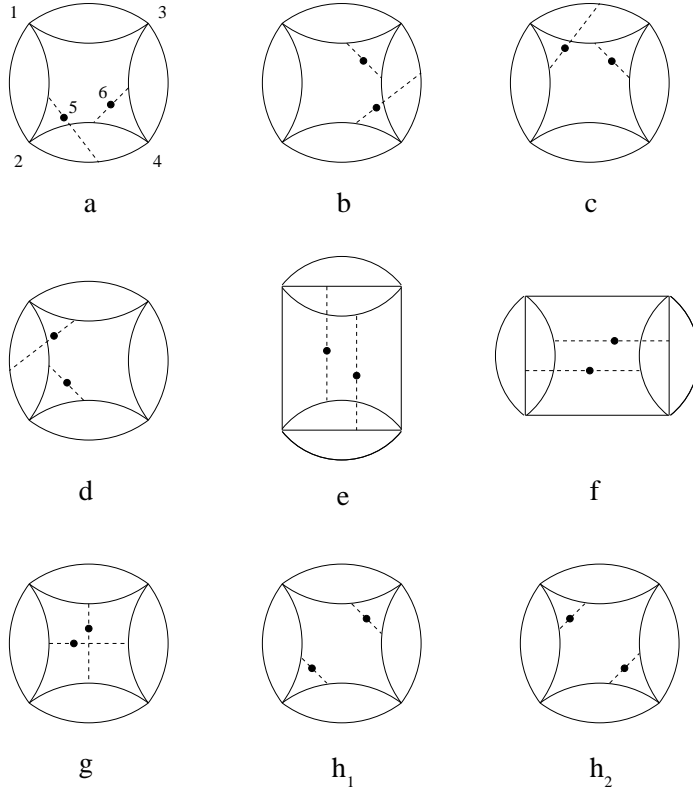


Figure 14. Diagrams contributing to the  $A_1$  function for  $k = 4$  case.

## References

- [1] J. Maldacena, “The large  $N$  limit of superconformal field theories and supergravity”, *Adv. Theor. Math. Phys.* **2** (1998) 231; G.G. Gubser, I.R. Klebanov and A.M. Polyakov, “Gauge theory correlators from noncritical string theory”, *Phys.Lett.* **B428** (1998) 105, hep-th/9802109; E. Witten, “Anti-de Sitter space and holography”, *Adv.Theor.Math.Phys.* **2** (1998) 253, hep-th/9802150.
- [2] A. M. Polyakov, “Gauge fields and space-time,” *Int. J. Mod. Phys. A* **17S1** (2002) 119, hep-th/0110196.
- [3] D. Berenstein, J. M. Maldacena and H. Nastase, “Strings in flat space and pp waves from  $N = 4$  super Yang Mills,” *JHEP* **0204** (2002) 013, hep-th/0202021.
- [4] S. S. Gubser, I. R. Klebanov and A. M. Polyakov, “A semi-classical limit of the gauge/string correspondence,” *Nucl. Phys. B* **636** (2002) 99, hep-th/0204051.
- [5] N. Beisert, C. Kristjansen and M. Staudacher, “The dilatation operator of  $N = 4$  super Yang-Mills theory,” hep-th/0303060.
- [6] J. A. Minahan and K. Zarembo, “The Bethe-ansatz for  $N = 4$  super Yang-Mills,” hep-th/0212208.
- [7] G. Arutyunov and E. Sokatchev, “On a large  $N$  degeneracy in  $N = 4$  SYM and the AdS/CFT correspondence,” hep-th/0301058.
- [8] O. Aharony, S. S. Gubser, J. M. Maldacena, H. Ooguri and Y. Oz, “Large  $N$  field theories, string theory and gravity,” *Phys. Rept.* **323** (2000) 183, hep-th/9905111.
- [9] E. D’Hoker and D. Z. Freedman, “Supersymmetric gauge theories and the AdS/CFT correspondence,” hep-th/0201253.
- [10] G. Arutyunov, F. A. Dolan, H. Osborn and E. Sokatchev, “Correlation functions and massive Kaluza-Klein modes in the AdS/CFT correspondence,” hep-th/0212116.
- [11] P. J. Heslop and P. S. Howe, “Four-point functions in  $N = 4$  SYM,” *JHEP* **0301** (2003) 043, hep-th/0211252.
- [12] A. Galperin, E. Ivanov, S. Kalitsyn, V. Ogievetsky and E. Sokatchev, “Unconstrained  $N=2$  Matter, Yang-Mills And Supergravity Theories In Harmonic Superspace,” *Class. Quant. Grav.* **1** (1984) 469; A. Galperin, E. Ivanov, V. Ogievetsky and E. Sokatchev, “Harmonic superspace”, Cambridge University Press, September 2001.
- [13] S. Penati, A. Santambrogio and D. Zanon, “Two-point functions of chiral operators in  $\mathcal{N} = 4$  SYM at order  $g^4$ ”, *JHEP* **9912** (1999) 006, hep-th/9910197; “More on correlators and contact terms in  $\mathcal{N} = 4$  SYM at order  $g^4$ ”, *Nucl. Phys. B* **593** (2001) 651, hep-th/0005223.
- [14] M. Bianchi, S. Kovacs, G. Rossi and Y. S. Stanev, “Anomalous dimensions in  $N = 4$  SYM theory at order  $g^4$ ,” *Nucl. Phys. B* **584** (2000) 216, hep-th/0003203.
- [15] B. U. Eden, P. S. Howe, A. Pickering, E. Sokatchev and P. C. West, “Four-point functions in  $N = 2$  superconformal field theories,” *Nucl. Phys. B* **581** (2000) 523 [hep-th/0001138].
- [16] F.A. Dolan and H. Osborn, “Conformal four point functions and the operator product expansion,” *Nucl. Phys. B* **599** (2001) 459, hep-th/0011040; “Superconformal symmetry, correlation functions and the operator product expansion,” *Nucl. Phys. B* **629** (2002) 3, hep-th/0112251.
- [17] B. Eden, A.C. Petkou, C. Schubert and E. Sokatchev, “Partial non-renormalisation of the stress-tensor four-point function in  $N = 4$  SYM and AdS/CFT,” *Nucl. Phys. B* **607** (2001) 191, hep-th/0009106.

- [18] B. Eden, C. Schubert and E. Sokatchev, “Three-loop four-point correlator in  $N = 4$  SYM,” *Phys. Lett. B* **482** (2000) 309, hep-th/0003096.
- [19] G. Arutyunov and S. Frolov, “On the correspondence between gravity fields and CFT operators,” *JHEP* **0004** (2000) 017, hep-th/0003038.
- [20] P. S. Howe, C. Schubert, E. Sokatchev and P. C. West, “Explicit construction of nilpotent covariants in  $N = 4$  SYM,” *Nucl. Phys. B* **571** (2000) 71 [hep-th/9910011].
- [21] B. Eden, C. Schubert and E. Sokatchev, “Three-loop four-point correlator in  $N = 4$  SYM,” *Phys. Lett. B* **482** (2000) 309 [hep-th/0003096];  
B. Eden, C. Schubert and E. Sokatchev, “Four-point functions of chiral primary operators in  $N = 4$  SYM,” Talk given at ‘Quantization, Gauge Theory and Strings’, Moscow, June 5-10, 2000 [hep-th/0010005].
- [22] B. Eden, C. Schubert and E. Sokatchev, unpublished.
- [23] G. Arutyunov, B. Eden, A. C. Petkou and E. Sokatchev, “Exceptional non-renormalization properties and OPE analysis of chiral four-point functions in  $N = 4$  SYM(4),” *Nucl. Phys. B* **620** (2002) 380, hep-th/0103230.
- [24] G. Arutyunov, S. Penati, A. C. Petkou, A. Santambrogio and E. Sokatchev, “Non-protected operators in  $N = 4$  SYM and multiparticle states of AdS(5) SUGRA,” *Nucl. Phys. B* **643** (2002) 49, hep-th/0206020.
- [25] G. Arutyunov, S. Frolov and A. C. Petkou, “Operator product expansion of the lowest weight CPOs in  $N = 4$  SYM(4) at strong coupling,” *Nucl. Phys. B* **586** (2000) 547 hep-th/0005182;  
“Perturbative and instanton corrections to the OPE of CPOs in  $N = 4$  SYM(4),” *Nucl. Phys. B* **602** (2001) 238, hep-th/0010137.
- [26] M. Bianchi, B. Eden, G. Rossi and Y. S. Stanev, “On operator mixing in  $N = 4$  SYM,” *Nucl. Phys. B* **646** (2002) 69, hep-th/0205321.
- [27] N. Beisert, “BMN operators and superconformal symmetry,” hep-th/0211032.